January 7, 1985

UNITED STATES OF AMERICA
NUCLEAR REGULATORY COMMISSION

Before the Atomic Safety and Licensing Appeal Board

In the Matter of	)	
	)	
LOUISIANA POWER & LIGHT COMPANY	)	Docket No. 50-382 OL
	)	
(Waterford Steam Electric Station, Unit 3)	)	

AFFIDAVIT OF JOSEPH L. EHASZ

Q1. Please state your name, address, and occupation.

A1. My name is Joseph L. Ehasz. I am employed by Ebasco Services Incorporated (ESI), Two World Trade Center, New York, New York 10048, as Chief Civil Engineer. A statement of my educational and professional qualifications is attached.

Q2. What has been your involvement in the Waterford 3 project?

A2. ESI, as Louisiana Power & Light Company's (LP&L) architect-engineer for the Waterford 3 project, has designed the plant structural system and has general management responsibility for construction, including the placement of all safety-related concrete. I have been involved in the Waterford 3 project since the inception of the design of the plant.

Q3. Has ESI analyzed the effects of the cracking in the Waterford 3 on the structural integrity of the basemat?

A3. Yes. Ebasco has studied closely and evaluated the results of the surface mapping and non-destructive testing (NDT) of the cracks. Ebasco has carefully studied the physical evidence of the cracks and evaluated this in light of the knowledge of soil properties and construction sequence to develop an understanding of the causes of cracking.

Ebasco has developed, from the NDT, a theoretical model of the cracks which was used in evaluating the effect of the cracks on the structural integrity of the basemat. Using this model and mathematical analyses, ESI evaluated the effects of the cracks on the flexural and shear transfer capabilities of the basemat and the effects of the cracks on the dynamic response of the structure.

The results of Ebasco's studies and analyses are described in the attached "Summary Evaluation - Structural Significance of Basemat Nondestructive Testing Results," Revision 2, November 27, 1984 (Attachment 1).

Q4. Has ESI come to a conclusion regarding the adequacy of the Waterford basemat?

A4. Yes. The Waterford 3 basemat cracks have been intensively studied for the past year and a half. Ebasco, as well as several consultants, have studied the physical location and geometry of the cracks and any ramifications on the structural integrity of the base mat which they could have. All have found them to be of no significance to the structural integrity of the basemat. The cracks have been mapped, measured and identified at depth by nondestructive testing means, the probable mechanism of their generation has been identified, and calculations have been made to predict their effect on the performance of the mat. All of these studies and investigations have led to the same conclusion that the cracks are of no significance to the structural integrity of the basemat and hence none to the safety of the plant under any of the postulated loading conditions.

As stated at page 23 of Attachment 1:

> [We] conclude that the cracks in the Waterford 3 basemat, as defined by the nondestructive testing, have no adverse influence on the structural integrity of the basemat. It is fully capable of functioning as required by the design in accordance with the pertinent codes.

Q5. Have you reviewed the affidavits submitted by the NRC Staff and Brookhaven National Laboratory to the Appeal Board on December 17, 1984, including the affidavit of John S. Ma and the views of John T. Chen as presented in Attachment 1 to the affidavit of James P. Knight?

A5. Yes, I have.

Q6. Are you in agreement with the conclusions of the NRC Staff and those of BNL?

A6. Yes, I agree with the conclusions of basemat adequacy presented by the Staff and the Brookhaven National Laboratory (BNL). In so doing, I concur with both the Staff and BNL in their disagreements with some of the views of Dr. Ma and Dr. Chen.

Q7. To what extent do you disagree with the views of Dr. Ma?

A7. Dr. Ma makes a number of statements which are inconsistent with the literature and the conventional body of engineering knowledge, including papers he himself has cited. However, my principal disagreement is with what appears to be his primary concern, that the cracks may significantly impair the capability for shear transfer of forces and the dynamic response of the basemat might be significantly changed.

With respect to shear transfer, Dr. Ma does not quantify the extent to which he believes that shear transfer will be impaired by the cracks, or even state positively that it will be a problem. Rather, he asserts, in general, with no attempt to relate his concern specifically to the characteristics of the basemat, that a crack will reduce the ultimate shear transfer strength and increase the slip due to load (Ma affidavit, page 26), and that "there has not been enough evidence to conclude that the existing cracks can be safely ignored" (Ma affidavit, page 31). The specific design aspects of the basemat, however, preclude such effects, a conclusion which is reflected in the expert views of the NRC Staff, BNL, and Professor Myle J. Holley, Jr.

The basis of Dr. Ma's concern appears to be a misreading of a paper which he cites by A. H. Mattock, et al., published in the PCI Journal, March-April 1972 (Ma affidavit, page 26). The paper is attached hereto as Attachment 2.1/ The basis cited by Dr. Ma is a quote from that paper that "'[a] pre-existing crack along the shear plane will both reduce the ultimate shear transfer strength and increase the slip at all levels of load.'" (Attachment 2, page 74.) That quotation, however, applies to a case where there is no compressive force on the crack, which is definitely not the situation for the Waterford 3 basemat.

Dr. Ma stopped short of noting that the Mattock paper also reports on results of testing for shear transfer across a crack when there is compressive force on the crack, such as exists at Waterford 3. The Mattock paper states:

> In a heavily reinforced shear plane, or one subject to a substantial externally applied normal compressive stress, it is possible for the theoretical shear resistance due to friction and dowel effects to become

---

1/ Dr. Ma has cited the wrong title of the paper. The title cited is a paper by Mattock, et al., which appeared in the July-August 1975 issue of PCI Journal, and which is not germane to this situation. Dr. Ma is clearly referring to the 1972 paper (Attachment 2).

> greater than the shear which would cause failure in an initially uncracked specimen having the same physical characteristics. In such a case, the crack in the shear plane "locks up" and the behavior and ultimate strength then become the same as for an initially uncracked specimen. (Attachment 2, page 70; see also page 75.)

The key element here is that the behavior in an initially cracked section can be the same as in an uncracked section if there is sufficient compressive force across the crack. The behavior referred to in the conclusion quoted by Dr. Ma is valid only in a section in which there is little or no compressive force across the crack. Then there must be initial slip to engage the reinforcing steel and develop tension in it, which is the very basis of shear-friction action. As noted at page 22 of Attachment 1 and at pages 21-22 of the July 18, 1984 BNL Report, the Waterford basemat has substantial compressive force across the cracks due to the externally applied soil and water pressures. Calculations were performed which showed that the maximum postulated shear was easily transmitted across the cracks utilizing the friction resulting only from the compressive force present on the crack faces. No utilization of extra compressive force brought by the reinforcing steel being engaged due to slight slipping of the crack faces is required. Thus, little or no slip will occur on the cracks due to transfer of shear under any of the design factored load conditions.

Dr. Ma's stated concerns with the lessons learned in the 1971 San Fernando earthquake regarding effect on bridges

(Ma affidavit, pages 17-18) has no bearing on the case at hand. The problem with the bridges had to do with expansion joints which were unreinforced and which were responding to large relative displacements high on a structure. The Waterford 3 basemat in no way resembles this situation, as it is an integrated reinforced concrete structure which is structurally continuous, with no expansion joints, and is supported on soil.

Similarly, Dr. Ma also provides a misleadingly partial quotation from a paper by Price to indicate that the basemat should be free of cracks:

> "[T]he primary requirement involved in mass concrete construction is that the completed structure is a monolithic mass that is free from cracks . . ." (Ma affidavit, page 30).

However, the complete quotation, and indeed, the article itself, clearly indicates that the statement applies to dams (which are not reinforced concrete structures), where freedom from cracks is important. The statement has no applicability to reinforced concrete structures, such as the basemat, where cracking is anticipated.

Q8. How do you disagree with Dr. Ma's concerns expressed at pages 16-18 and 31 that the cracks will cause deviations from the predicted seismic response of the basemat?

A8. Dr. Ma's concern that the seismic response will deviate because of the cracks, and that the significance of such deviation is not known (Ma affidavit, page 18), appears to arise from his asking us to assume "that the crack is wide and there is no contact between concrete surfaces across a crack." (Ma affidavit, page 17). Such an assumption is clearly erroneous, as discussed above, because of the substantial compressive force across the cracks in the Waterford 3 basemat. Moreover, Dr. Ma does not identify the forces which would separate the faces of the crack to eliminate contact. In fact, there are no such forces. Further, actual measurements of cracks at surface and at depth show them to be of modest width.

Since it has been demonstrated that the shear behavior of the mat will not be significantly affected by the cracks, and since no significant increase in the flexure of the basemat will be caused by the cracks (Attachment 1, pages 15-16), it follows that the dynamic response of the mat will not be significantly affected by the presence of the cracks.

Dr. Ma has noted that the dynamic response of the basemat was determined using a model which assumed that the mat behaved as a single monolithic structure. (Ma affidavit, page 16.) He noted that the model was valid with shallow cracks present, but questioned the validity of the model if the deeper cracks in the basemat are present. In fact, the basemat cracks do not invalidate the model. As discussed above, the cracks do not affect the shear and flexural behavior of the mat. The cracked mat therefore can be correctly assumed to act monolithically. Hence, the cracks have no significant effect on dynamic response of the basemat. See Attachment 1, pages 16, 22-23.

A dynamic analysis performed by BNL is a demonstration of the small effect that total elimination of the shear transfer capability in one element of the basemat could have. (Affidavit of Reich, et al., Attachment 1, Appendix D.) The analysis shows that the response of the structures above the mat is virtually unaffected, even by the assumption of such a fictitious loss of mat rigidity.

Q9. Do you share Dr. Ma's concerns expressed at page 28 of his affidavit about steel corrosion and durability?

A9. It is not clear to me that Dr. Ma has actually expressed such a concern about the Waterford 3 mat specifically. He discusses the general concepts of rebar corrosion and concrete durability, but does not define any specific concerns applicable to the basemat. In any event, the record is clear that we have no problems with corrosion and durability in the Waterford 3 basemat.

The cracks as they exist at present are not leaking any appreciable amount of water. At some spots, a dampness marks the location of the crack, but otherwise the cracks are dry at the surface. This indicates that there has been a healing or filling of the crack sufficient to prevent about a 50-foot head of water from forcing water through them. Any water in the cracks has become stagnant and alkaline in nature, which makes it noncorrosive. Nevertheless, extensive studies were performed to identify the corrosion hazard to the reinforcing steel in the mat and to ascertain if there would be any hazard to it during the life of the plant.

In his affidavit of September 27, 1983, submitted in support of LP&L's answer to the earlier motion to reopen on the basis of basemat cracks, William Gundaker, ESI Director of Corrosion Engineering, reviewed and summarized these studies and the results and conclusions. He stated at page 6 of his affidavit that ". . . I can state that there is no reason for me to believe that corrosion of the reinforcing steel in the concrete mat at Waterford 3 Nuclear Plant would occur to a degree that would have any significance." This statement was made after a series of chemical tests on the water which was extracted from a crack and from water which was extracted from the ground adjacent to the mat, and an examination of the results of these tests in light of a clear understanding of the potential causes of corrosion in reinforcing steel embedded in concrete.

We have also looked at the experience with concrete structures in the vicinity of the plant. Ebasco has put in place many concrete structures and foundations in the general area of the Waterford Plant in the last 50 years with no reported failures due to corrosion of reinforcing steel. In all of these structures the general design and stress levels are about the same as those at Waterford.

Q10. Do you find any significant disagreement among the various views presented, including those of Dr. Ma and Dr. Chen, on the cause of the basemat cracks?

A10. No, I do not see any significant disagreement among the current views put forth as to the cause of the cracks. All who have expressed their views appear to agree that the primary cause was differential settlement of the basemat during construction, as well as the normally expected thermal shrinkage.

The causes for the cracking in the Waterford basemat have been determined to be from two interrelated reasons -- the highly compressible nature of the soil beneath the plant and the sequence of construction of the basemat.

The soil beneath Waterford is a normally consolidated clay, silt and sand mixture which was laid down by water in the Pleistocene Age. It is horizontally bedded and generally quite compressible when loads in excess of those which it has experienced in the past are impressed upon it. The Waterford mat, during the early construction phases, imposed such loads upon it and hence consolidation was expected and was experienced. The method of impressing this load was controlled under engineering direction by strict control of the construction sequencing of the mat and superstructure.

The basemat, which is 267 feet by 380 feet, was necessarily constructed by the sequential placement of 60-foot by 70-foot blocks. The blocks are structurally continuous. The construction sequence resulted in a staged consolidation of the Pleistocene soils such that the north and south ends of the mat have settled more than the center where the construction started. Much of the settlement of each block occurred soon after concrete placement, with the rate of settlement tapering off with time. Thus, the first block of the basemat placed had experienced an initial settlement by the time an adjacent block was placed. The adjacent block was placed level with the previously placed block, and then underwent settlement starting at the level of the already partially settled first block. Thus, the second block had to undergo all of its settlement while the first block only had a percentage left to go. While the total settlement for each block was about equal, because placement of the basemat was done from the center outward to the north and south ends, the result was a mat which was finally convex up with the highest portion being at the center of the reactor building. Figure 2 of Attachment 1 illustrates this shape of the basemat.

The convexity of the basemat resulted in tensile forces due to flexure at the top of the basemat in the middle section early in the life of the mat. This resulted in the cracking. As illustrated in Figure 2 of Attachment 1, the flexure was greatest around the reactor building centerline and was quite symmetric to the north and south. The cracking is predominantly in an east-west orientation and concentrated around the east-west reactor building centerline.

With the addition of superstructure loads, the flexure of the mat was reduced as it was stressed more in accordance with the final loading conditions. This put the top of the mat in compression and closed up the cracks.

Both Dr. Ma (Ma affidavit, page 1) and Dr. Chen have expressed disagreement with BNL on the cause of the cracking. This is apparently because each of them has referred to an early conclusion of BNL (July 18, 1984, BNL Report, page 26) that the cracking was largely due to the placement of loads on the constructed basemat by construction of the plant superstructures prior to the placement of backfill. However, from discussions with BNL, it became apparent that BNL was initially under a mistaken impression about the sequence of construction. After learning that the soil backfill was not placed after construction of the superstructures, BNL modified its conclusion and now agrees that the cause of the cracking was primarily due to differential settlement during placement of the basemat (Affidavit of Reich, et al., Attachment 1, page 3).

With all parties agreeing fundamentally on the cause of the cracking, the only remaining difference of opinion seems to be related to the precise soil mechansim which caused the differential settlement to occur.

Q11. What is the difference of opinion regarding the soil mechanism leading to the differential settlement?

A11. Contrary to the positions of Ebasco, the NRC Staff, and BNL, Dr. Ma and Dr. Chen suggest that the differential settlement may have been due to non-uniformity of the soil beneath the basemat. Soil non-uniformity, however, is not necessary for differential settlement of the mat to have occurred. In fact, as I discussed in my answer to Question 10 above, even though the soil was relatively uniform, differential settlement was anticipated, and the construction sequences was planned to minimize and maintain symmetry of the differential settlement.

The postulation of non-uniform soil is contrary to the objective evidence. First, extensive preconstruction soil tests showed the soil beneath the basemat to be uniform. At the Waterford site, 74 soil borings were drilled. Of these, 22 were in the area of the basemat. Numerous soil tests were performed on the Pleistocene clays, giving results that show similarity in grain size distribution and relative uniformity in strength, permeability, and compressibility. Following excavation, which exposed the upper several feet of the Pleistocene formation, the soil was mapped in detail. The formation at foundation level consists of horizontally bedded layers of silts and clays. The conditions encountered compare very favorably with the data taken from the site borings. Mapping of the excavation disclosed no abnormalities or discontinuities in the foundation materials.

Second, the relatively symmetric differential settlement experienced by the basemat is indicative of relatively uniform soils. Non-uniform soils would not lead to the symmetric settlement pattern exhibited by the basemat with its carefully sequenced construction. It is not conceivable that such symmetric settlement would have occurred with non-uniform soils.

Finally, the cracking pattern itself was consistent with the symmetric settlement which could not have occurred over non-uniform soils. The pattern of cracking in plan is not a random one, but rather a pronounced east west alignment strongly concentrated around the east west centerline of the reactor building and somewhat symmetric with the centerline. The cracks are predominantly near or emanating from the top surface of the mat and are all vertical as defined by non-destructive testing (NDT) methods.

Q12. Does it really matter whether the differential settlement occurred over uniform or non-uniform soils?

A12. No, I do not believe so, because the differential settlement has essentially stopped. Dr. Ma appears to agree:

> . . . the possible major contributing factors to the cause of the cracks would have vanished and would not appear again. Thermal stress due to the cement hydration process, which might have produced the cracks, would not appear again. Stress resulting from concrete block construction sequences has leveled off. Stress associated with differential settlements decreases as the settlements of soils became stabilized through soil consolidation process. The significant groundwater level changes during construction would not reappear. (Ma affidavit, page 31).

While Dr. Ma prefaced these observations with a recommendation that the cracks be repaired, his stated reasons for believing that the causes of the cracks had vanished are unrelated to whether or not the existing cracks are repaired.

Similarly, Dr. Chen at page 9 concluded that

> The plant foundation design, the "compensated" foundation concept, is sound and acceptable. The soil bearing capacity is adequate and the future settlement should be negligible.

Our analyses, as confirmed by our monitoring of basemat settlement, show that future settlement of the basemat, if any, will be insignificant, irrespective of the uniformity or non-uniformity of the underlying soils. The existing cracks, caused primarily by the differential settlement which resulted in a convexity at the top of the basemat with commensurate tensile stresses over the top surface, have been closed by the placement of the plant superstructure deadload on the basemat. The significance of these cracks on the structural adequacy of the basemat has been determined, and it is no longer of significance what the exact causes of the cracks were, other than to determine that the causes are no longer active.

Joseph L. Ehasz

JOSEPH L. EHASZ

Subscribed and sworn to before me this 7th day of January, 1985.

Josephine R. Bambara

NOTARY PUBLIC

Josephine R. Bambara
Notary Public, State of New York
No. 52-5166015
Qualified in Suffolk County
Certificate filed in New York County
Commission Expires March 30, 1986

My Commission Expires: ______________

JOSEPH L. EHASZ

Chief Consulting Civil Engineer

EXPERIENCE SUMMARY

Registered Professional Engineer in sixteen states with seventeen years of experience in civil engineering, design and construction aspects of major hydroelectric, fossil-fueled and nuclear generating stations. Major field of interest is in civil and geotechnical related aspects of power plant structures; in particular the soil and rock mechanics design, analysis and construction of earthworks and foundations for dams, embankments, and major plant facilities.

Responsible to the Vice-President of Consulting Engineering for all technical, administrative and personnel aspects of the Consulting Civil Engineering and Earth Sciences Departments. Responsibilities have included direction of civil engineers as well as the soils engineering group working on foundation engineering and design features of hydroelectric and steam power stations; supervision of engineers working on all civil aspects of power stations as well as directing engineers with respect to soils and field reconnaissance investigations, establishing foundation design criteria, establishing earthquake design criteria, engineering on design drawings and construction specifications.

Office assignments have included lead civil engineer on various hydroelectric and steam electric power stations. Geotechnical experience includes design and analysis of difficult foundations, detailed stability and settlement analyses for unusual subsurface conditions designing and analyzing large earth and rockfill dams and developing observation systems for earth and rockfill dams. Work includes establishing foundation design criteria for nuclear power plants, entailing both static and dynamic factors and considerations; the analysis of the various foundation types and the effects on the dynamic considerations of the building components. Job engineering includes civil engineering features such as channels, dikes, general fuundation layout of steam electric stations, transmission lines and river crossings. Responsible for the engineering of a 15-mile makeup pipeline and associated reservoir and river pumping facilities, including site investigation and reservoir embankment and spillway design. Responsibilities also included engineering on foreign hydroelectric projects involving detailed geotechnical studies, dam foundation evaluation and associated foundation treatments for a 500-foot arch dam and a 680-foot high rockfill and concrete gravity dam complex.

Field assignments have included supervision on field investigation, borings and test pits for hydroelectric nuclear and steam electric plant sites; inspection of construction associated with waterfront docking facilities; supervision and inspection on caisson construction, pile driving and pile load testing on various plant sites. Field supervision to establish criteria for controlled compacted backfill for soil bearing foundations and responsible charge of detailed seepage studies for pumped storage projects, including field assignments during initial filling of upper and lower reservoirs. Responsible for site evaluation and grouting programs developed for varied embankment dams as well as concrete dams.

JOSEPH L. EHASZ

REPRESENTATIVE EXPERIENCE

Client	Project	Size	Fuel
Arizona Public Service Company	Cholla Unit Nos. 1, 2, 3 & 4	115 MW 250 MW 250 MW 400 MW	Coal
Dallas Power & Light Company	Lake Hubbard Unit No. 1	375 MW	Gas
Houston Lighting & Power Company	Cedar Bayou Unit Nos. 1 & 2	750 MW ea.	Oil/Gas
Pennsylvania Power & Light Company	Brunner Island Unit No. 3	790 MW	Coal
	Montour Unit Nos. 1 & 2	800 MW ea.	Coal
Portland General Electric Company	Bethel Unit No. 1	100 MW	Gas Turbine
	Harborton	200 MW	Gas Turbine
	Beaver	450 MW	Gas Turbine
United Illuminating Company	Bridgeport Harbor Unit No. 3	400 MW	Coal
Carolina Power & Light Company	Shearon Harris Unit Nos. 1, 2, 3 & 4	960 MW ea.	Nuclear
Florida Power & Light Company	St. Lucie Unit Nos. 1 & 2	890 MW ea.	Nuclear
Houston Lighting & Power Company	Allens Creek Unit No. 1	1200 MW	Nuclear
Louisiana Power & Light Company	Waterford Unit No. 3	1165 MW	Nuclear
Washington Public Power Supply System	WPPSS Unit Nos. 3 & 5	1300 MW ea.	Nuclear

JOSEPH L. EHASZ

EMPLOYMENT HISTORY

Ebasco Services Incorporated, New York, N.Y.; 1965 - Present

- o Chief Consulting Civil Engineer, 1980 - Present
- o Corporate Chief Civil Engineer, 1979-1980
- o Assistant Chief Civil Engineer, 1977-1979
- o Supervising Engineer, 1971-1977
- o Engineer, 1965-1971

Rutgers University, College of Engineering, Graduate School, New Jersey; 1964-1965

- o Graduate Student and Teaching Assistant;

Burns & Roe, Inc., Engineers and Constructors, New York, N.Y.; 1963-1964

- o Engineer

EDUCATION

Rutgers University, New Jersey - BSCE - 1963
Rutgers University, New Jersey - MSCE - 1965

REGISTRATIONS

Professional Engineer - New Jersey, Alaska, Arizona, California, Florida, Georgia, Louisiana, Michigan, Minnesota, New York, North Carolina, Pennsylvania, Texas, Washington and West Virginia.

PROFESSIONAL AFFILIATIONS

American Society of Civil Engineers
American Concrete Institute
International Society of Soils & Foundation Engineers
International Commission on Large Dams
Committee on Earthquakes
New Jersey Society of Professional Engineers
Rutgers Engineering Society
Who's Who In Engineering (1982)

JOSEPH L. EHASZ

TECHNICAL PAPERS

"Static and Dynamic Properties of Alluvial Soils in the Western Coastal Plain of Taiwan"; co-authored with K.Y.C. Chung; 7th Southeast Asian Geotechnical Conference; Hong Kong, November 1982

"Experience with Upstream Impermeable Membranes" 14th ICOLD Congress, Rio de Janeiro, May 1982

"Ash Pond Construction to Meet Performance Requirements"; co-authored with M Temchin, ASCE Convention & Exposition, New York, NY, May 1981

"Foundation Movements - Prediction and Performance"; co-authored with M Pavone; 10th International Conference on Soil Mechanics and Foundation Engineering; Stockholm, Sweden, 1981

"Dynamic Properties of Weathered Rock"; co-authored with I H Wong & K H Liu, 7th World Conference on Earthquake Engineering; Istanbul, Turkey; Sept 1980

"Probability of Liquefaction due to Earthquakes", co-authored with I H Chou, 7th World Conference on Earthquake Engineering; Istanbul, Turkey; Sept 1980

"Liquefaction Considerations in Nuclear Power Plant Design" ASCE Specialty Conference on Structural Design of Nuclear Power Foundations, New Orleans, December 1975.

"Experience on Dams with Upstream Impermeable Membranes", Conference on Recent Developments in Design, Construction and Performance of Embankment Dams, University of California at Berkeley, June 1975.

"Compatibility of large Mat Design to Foundation Conditions," ASCE National Structural Engineering Convention, New Orleans, April 1975.

"The Effects of Foundation Conditions on Plant Design," Atomic Industrial Forum, San Diego, December 1974.

"Implementation of Foundation Design Criteria", ASCE Specialty Conference on Structural Design of Nuclear Plant Facilities, Chicago, December 1973.

"Foundation Design of the Waterford Nuclear Plant", ASCE Specialty Conference on Structural Design of Nuclear Power Facilities, December 1973.

"Civil Engineering Aspects of the Montour Steam Electric Station", Pennsylvania Electric Association, October 1970.

"Civil Engineering Aspects of Brunner Island Unit No. 3, Foundation and Circulating Water System", Pennsylvania Electric Association, May 1967.

ATTACHMENT 1

LOUISIANA POWER & LIGHT / 142 DELARONDE STREET • P.O. BOX 6008
NEW ORLEANS, LOUISIANA 70174-6008 • (504) 366-2345
MIDDLE SOUTH UTILITIES SYSTEM

November 28, 1984

W3P84-3319
3-A1.16.07
A4.05

Director of Nuclear Reactor Regulation
ATTN: Mr. Dennis M. Crutchfield, Asst. Director
for Safety Assessment
Division of Licensing
U.S. Nuclear Regulatory Commission
Washington, D. C. 20555

SUBJECT: WATERFORD 3 SES
ADDITIONAL INFORMATION ON BASEMAT
HAIRLINE CRACKS

References: Letter W3P84-3142, K. W. Cook to D. M. Crutchfield, dated November 7, 1984.

Dear Mr. Crutchfield:

The purpose of this letter is to supplement the additional information provided in the referenced letter. This information was requested by the NRC and Brookhaven National Laboratory personnel at a meeting in Bethesda, Maryland on November 20, 1984.

Attached is Revision 2 of the report entitled "Summary Evaluation Structural Significance of Basemat Nondestructive Testing Results". This revision addresses questions discussed among parties at the November 20, 1984 meeting. Further information regarding the degree of confidence in NDT results, probable causes of cracks, mechanisms for deep narrow cracking, construction controls, shear considerations, slip resistance, etc.

Louisiana Power & Light remains firmly convinced that the cracks, as defined by NDT have no adverse affect on the structural integrity of the basemat. The basemat is fully capable of functioning as required by the design in accordance with the pertinent codes.

Very truly yours,

K. W. Cook by [illegible]

K. W. Cook
Nuclear Support & Licensing Manager

KWC:plc

ATTACHMENT

cc: E.L. Blake, W.M. Stevenson, G.W. Knightou, J.M. Knight, J.H. Wilson
G.L. Constable, Project Files, Administrative Support, Licensing Library

LOUISIANA POWER AND LIGHT COMPANY
WATERFORD STEAM ELECTRIC STATION
UNIT NO. 3

SUMMARY EVALUATION
STRUCTURAL SIGNIFICANCE OF BASEMAT
NONDESTRUCTIVE TESTING RESULTS

REVISION 2*

November 27, 1984
Ebasco Services Incorporated
Two World Trade Center
New York, NY 10048

*Includes revisions, clarifications and additions to the Revision 1 Report of November 1984 based on the November 20, 1984 meeting with NRC staff and Brookhaven National Laboratory.

LOUISIANA POWER AND LIGHT COMPANY

WATERFORD STEAM ELECTRIC STATION

UNIT NO. 3

SUMMARY EVALUATION

STRUCTURAL SIGNIFICANCE OF BASEMAT

NONDESTRUCTIVE TESTING RESULTS

TABLE OF CONTENTS

		Page
1.0	PURPOSE	1
2.0	SCOPE	1
3.0	BACKGROUND	1
4.0	NDT RESULTS SUMMARY	2
5.0	PROBABLE CAUSES OF CRACKS	9
6.0	SIGNIFICANCE OF CRACKS AND EFFECTS ON STRUCTURAL INTEGRITY	13
7.0	CONCLUSION	23
REFERENCES		24

TABLE 1 - SUMMARY OF CRACKS WEST SIDE OF RCB

TABLE 2 - SUMMARY OF CRACKS EAST SIDE OF RCB

TABLE 3 - SUMMARY OF CRACKS BENEATH RCB

TABLE 4 - SUMMARY OF CRACKS IN RCB WALLS

FIGURE 1 - BASEMAT CRACKS - PLAN VIEW

FIGURE 2 - BASEMAT CURVATURE (From Reference 2)

APPENDIX 1 - REINFORCING STEEL STRESSES AS DEFINED BY CRACK WIDTH (CALCULATION)

LOUISIANA POWER AND LIGHT COMPANY

WATERFORD STEAM ELECTRIC STATION

UNIT NO. 3

SUMMARY EVALUATION

STRUCTURAL SIGNIFICANCE OF BASEMAT

NONDESTRUCTIVE TESTING RESULTS

1.0 PURPOSE

The purpose of this report is to review the results of nondestructive testing (NDT) of Nuclear Plant Island Structure (NPIS) basemat cracks and to evaluate their significance with respect to the structural integrity of the NPIS.

2.0 SCOPE

The scope of this report covers the following:

1. Review and interpret data and results of NDT related to basemat as presented in the Muenow and Associates, Inc. Report of October 1984 and Appendix 6 of that report which was issued November 13, 1984.

2. Evaluate the significance of the cracks on the structural integrity of the NPIS basemat.

3. Study the crack patterns as defined by NDT, such as inclination, depth, spacing, and width in order to determine the probable causes of basemat and wall cracks.

3.0 BACKGROUND

An NDT program of the basemat cracks was performed by Muenow and Associates, Inc. to determine the following:

1. Inclination of the cracks - whether the basemat cracks are vertical and/or diagonally inclined.

2. Estimate depth, length, and width of the basemat cracks.

As an auxiliary study, the depth of some cracks of the Reactor Containment Building (RCB) wall surfaces above the basemat was evaluated.

This NDT examination was performed at the Waterford 3 Site mainly during the months of July and August 1984.

4.0 NDT RESULTS SUMMARY

4.1 CRACKS IN BASEMAT (Tables 1, 2 and 3)

The majority of the cracks are oriented in an east-west direction and located within a distance of thirty (30) feet from the east-west centerline of the RCB. Based on their appearance and nearness to each other they are grouped into 10 families:* 4 on the east side of the RCB and 6 on the west side of the RCB. Seven cracks beneath the RCB were also identified by NDT, four of these cracks (Numbers 1, 4, 5 and 7) appear to coincide with east-west cracks on either side of the RCB and probably are interconnected (Figure 1).

Other cracks are oriented in a northeast/southwest or northwest/southeast direction (diagonal cracks) and they are grouped into a total of 7 families. Of these families, 4 were evaluated by NDT: 3 in the northeast and 1 in the northwest corners of the RCB. These cracks are also referred to as East or West Diagonal cracks in the Muenow and Associates, Inc. Report. Two of the cracks beneath the RCB (Numbers 2 and 6) appear to coincide with the East or West Diagonal cracks and probably are interconnected (Figure 1).

*The grouping by families is somewhat arbitrary and intended only to present an overview of the mat cracking. No analyses or conclusions are dependent upon the grouping.

One crack, number 3, appears to be independent of all others and is relatively short in length.

Ebasco review indicates that within the above families of cracks, the data show most cracks originate from the top surface of the basemat (top cracks), that a few noncontinuous cracks originate from the bottom surface of the basemat (bottom cracks), and a small number lie within the middle portion of the basemat (middle cracks).

Tables 1 and 2 present a summary of the NDT examination of the basemat cracks on each side of the RCB. This includes length, depth, group spacing and inclination of cracks which originate from the top surface of the basemat. In addition, a summary of cracks in the middle or near the bottom of the basemat is included.

Table 3 presents a summary of cracks beneath the RCB. These cracks are oriented mainly in the E-W direction.

4.1.1 Depth

East-West Cracks Outside RCB

The depth of the top cracks varies depending on the locations of the cracks. Generally, individual cracks do not extend into the bottom region of reinforcing steel located approximately ten (10) feet depth from the top surface.

The neutral axis for positive bending (tension at top surface of the basemat) is calculated to be approximately 10'-6 from the top surface. The total basemat thickness is 12'-0.

The bottom cracks are found mostly in the vicinity of the east-west centerline of the RCB and their depths range from 2 to 3 feet, measured from the bottom of the basemat. Within this area a possible local interconnection between top and bottom cracks is indicated for Cracks J and Ke.

4.1.1 Depth (Cont'd)

East-West Cracks Outside RCB (Cont'd)

The middle cracks are randomly distributed. In general, they are not interconnected with top or bottom cracks.

Cracks Beneath the RCB

The interpretation of the crack depths beneath the RCB reflects the difficulties of extending the NDT technique to such long distances. Differing interpretations have identified these cracks as being noncontinuous and variable in depth, and also as being continuous and rather continuously extending to near the bottom of the basemat.

Diagonal Cracks (Northeast/Southwest and Northwest/Southeast)

The depth of these cracks, which in plan view run diagonally to the plant grid, is generally less than six (6) feet. A few bottom and middle cracks are present, however, there are no indications of interconnection between the top and bottom cracks.

4.1.2 Inclination

All cracks in the basemat evaluated by NDT are essentially vertical. In Page 2, of the Muenow and Associates, Inc. report it is stated that "there is no evidence of diagonal (shear) cracks; either occurring singularly or as a connection between two individual cracks within the areas investigated."

4.1.3 Length

The cracks are variable in their length. The east-west cracks outside the RCB extend between the exterior wall of the RCB and the wet cooling tower walls. In the one case where visible and accessible for NDT examination, family VI-cracks U, V, X, the cracks extend to the area of the external walls of the NPIS. The diagonal cracks extend from the

4.1.3 Length (Cont'd)

exterior wall of the RCB but end well before they reach the exterior wall of the NPIS. When the cracks intersect with a construction joint they go through the construction joint. It appears that there are 6 cracks that extend from the east to the west side of the NPIS basemat since many of the individual families located in three areas (east, west and beneath the RCB) coincide and are probably joined.

4.1.4 Spacing

The east-west crack families have an average spacing of approximately 11'-0. The diagonal (north-east/southwest or northwest/southeast) crack families have an average spacing of approximately 15'-0 at the exterior wall of the RCB.

4.1.5 Width

The NDT evaluation has estimated the crack width to be less than .007 in. and all the cracks are tight. Our recent field surface measurement of crack L, done coincidentally with NDT examinations found the maximum crack width to be .003 in. The crack was observed to be filled with laitance and there was no actual open crack. Our field surface measurements in 1977 found the crack widths beneath the RCB to be between .002 and .005 in. Cracks of this width are commonly referred to as "hairline" cracks. Field measurements were made using a Bausch & Lomb optical comparator.

4.1.6 Evaluation of Confidence in NDT Results

As a result of a consideration of the techniques used in performing the NDT examination of the basemat cracks and the procedures utilized in evaluating the data derived from the NDT with respect to confidence in the accuracy of the reported crack information we conclude:

1. Outside RCB

The ability to work close to the surface crack indication leads to a high confidence level in the location and orientation of the tested cracks. A somewhat lower, but still high, confidence level is associated with the location of the bottom of the cracks and a slightly lower confidence in the crack width measurements.

a. Location and Orientation of Crack

The location and orientation of the cracks is dependent upon the accuracy of the location of the transducer and the accuracy and precision of the measurement of time. Since both of these can be, and were, closely controlled and not subject to great variation or subjective interpretation there is high confidence that the location and orientation of the cracks are as defined by the NDT.

b. Depth of Cracks

Due to the divergence of the sound waves used in the testing, a precision of 1 ft in the location of the bottom of the cracks is recognized by Muenow(1). This, since the cracks generally extend down from the top of the mat, leads to a conclusion that the actual bottom of the crack can be as much as one foot above the bottom as defined in the Muenow Report, where the latter is defined at the center of the diverging cone. Therefore, the depth of the cracks outside the RCB are no deeper than and could be as much as one foot less than the values reported by Muenow.

c. Width of Crack

The measurement of crack width is not an exact measurement according to the Muenow report, but is an estimate only. Muenow assigns an accuracy of 20% to the value he reports ($\lesssim$7 mils), which essentially means he is reporting the cracks

(1) Muenow Report, p. 16

c. Width of Crack (Cont'd)

to be less than 8-1/2 mils. This together with the independent measurement of the surface crack width of 3 mils gives confidence that the cracks are all quite narrow (on the order of 5 mils).

2. Beneath RCB

The technique used beneath the RCB involving greater distances from transducer to crack and requiring several reflections from the top and bottom of the mat results in a lower confidence level for some of the results derived therefrom.

a. Location and Orientation of Cracks

The location and orientation of cracks using a 60° transducer and several reflections from the mat top and bottom is dependent upon the accuracy of the location of the transducer and the measurement of time. Since these were closely controlled, the confidence in the NDT defined location and orientation is high.

b. Depth of Crack

The confidence level in the validity of the data defining the depth of cracks beneath the RCB is substantially below that for the cracks outside the RCB. There appears to be a large measure of subjective analysis and intuition injected into the interpretation of the raw data to determine the crack depth.

2. Beneath RCB (Cont'd)

b. Depth of Crack (Cont'd)

As with the 45° transducer data, the divergence of the sound waves causes a diminishing of the precision of the data. A 2 to 2-1/2 ft precision is quoted by Muenow which may be enhanced by interpretation of frequency content and amplitude. The precision quoted is open to question and the nature of the enhancements is not clearly defined. While such refinements are theoretically possible, they are not demonstrated, and hence must be discounted, resulting in less confidence in the accuracy of the depth of cracks as reported is valid. This lack of confidence renders uncertain whether the cracks are truly as deep as reported.

However, for reasons cited earlier, whatever the uncertainty regarding interpretation of the crack depths, the cracks are never deeper than reported.

In summary, the location and orientation of the cracks, which are the aspects of greatest significance, are known with a high degree of confidence. The width and depth, which are of lesser significance, are known with a lesser confidence.

4.1.7 Crack Model for Evaluation

As a result of this evaluation of the confidence in the reported NDT testing and evaluation, the following model of the basemat cracks can be drawn:

The basemat cracks are vertical, or nearly so, and generally extend down from the top of the mat at locations where there are top surface indications of a crack. This orients them generally in an east-west direction. They appear to extend in many cases almost completely across the mat. They extend down a variable depth, in some cases to the region of the bottom reinforcing steel. The actual depth of the cracks is questionable along much of the length beneath the RCB, and hence an assumption for conservatism will be made, in the evaluation of their significance, that they extend from the top to the bottom of the mat. It is cautioned that this simplifying conservative assumption is demonstrably not the case for a significant portion of each crack and such assumption is made simply for purposes of ease of evaluation. The crack widths are quite narrow, on the order of 5 mils, and, by visual observation at the top of the mat, filled with a laitance material and not open.

4.2 CRACKS IN RCB WALL

Four hairline cracks on the exterior surface of the RCB wall near the basemat (Elev -35.0 ft) were evaluated using NDT. All of them were found to penetrate less than one (1) ft of the 10 ft wall thickness (Table 4).

5.0 PROBABLE CAUSES OF CRACKS

The causes of the top cracks were evaluated in 1977 and 1983 (Reference 1) and the conclusion was that they were mainly due to flexure of the basemat from initial loading (prior to the completion of superstructure). The NDT evaluation has determined that all of the top cracks are vertical, extremely narrow and do not generally extend below the neutral axis.

Although the predominant cause of cracks has been concluded to be flexure, other factors such as thermal and/or shrinkage strains probably contributed to their development. Also, the early placement of the lower portion of the RCB ring wall apparently influenced the cracking orientation as evidenced by the radial nature of the most northerly and southerly cracks.

5.1 CRACK PATTERN

From the summary of NDT results, it is clear that the top cracks are greater in number than the bottom cracks. This reflects that the crack pattern generally followed the basemat flexure, which was found to be predominantly convex shape throughout the construction stages. The top cracks are located primarily in an east-west band centered on the RCB centerline. This matches closely the area of maximum convex flexure of the basemat in the early stages of construction as shown on Figure 2.

The causes for the convex flexure of the basemat during construction were the sequence of construction of the basemat blocks for the basemat and the different rates of settlement of the foundation soil beneath each placement block. While the soil beneath the entire basemat is uniform, the loading imposed upon it was placed in segments at different times (each placement block being a loading segment). Thus, the soil beneath each placement block followed the same time-consolidation curve but at a different location on the curve because of the different placing times. As a result, the differential settlement between the last block placed and the first placed was greater than that between those placed earlier and the first. This caused a convex shape to the mat with the earliest blocks placed, at the center of the RCB, being at the top of the convex shape (see Fig. 2). The present convexity is very small being 2-1/2 inches over 380 feet. To prevent any excessive or eccentric differential settlement of the basemat, engineering controls on the placement sequence of the superstructure were utilized. This assured nearly uniform superstructure dead loading on the mat at all times during construction.

5.2 CRACK WIDTH AND DEPTH

The present crack widths are well within the allowable crack width of the ACI Codes. Section 1508.6, ACI 318-63 Code for control of cracking states that "....the average crack width at service load at the concrete surface of extreme tension edge, does not exceed 0.010 in. for exterior members..." Section 10.6.4, ACI 318-83 Code Commentary for control of flexure cracking states that "...for interior and exterior exposure respectively, ... limiting crack widths of 0.016 and 0.013 in."

The NDT examination performed at service load conditions has established the estimated crack width to be less than .007 in. and the actual field measurements of crack "L" less than .003 in. When the basemat cracks were first observed under the RCB in mid-1977, the crack widths were observed to be between .002 and .005 in. The tensile stress in the top reinforcing steel which would correspond to these observed crack widths (approximately .005 in.) is small, on the order of 11 ksi, well within the allowable design limits (Appendix 1). The design yield strength of the reinforcing steel is 60 ksi.

In Reference 1, it was stated that "...The mat, as are all other reinforced concrete structures, is designed to carry loads and in so doing depends only on the compressive and shear strengths of concrete and the tensile strength of reinforcing steel. No credit is taken in the design for the tensile strength of concrete, ... Thus, as loading on the foundation mat causes flexure and resultant tension of the concrete, cracks are expected to form. This cracking enables transfer of the tensile load from the concrete to the embedded reinforcing steel as contemplated in the design of all steel reinforced concrete structures."

The positive and negative bending capacities of the mat are in no way diminished by the presence of the flexural cracks which are essentially vertical and which are of very modest width. Neither are the bending capacities in any way diminished by the depth of cracks, even if the cracks are assumed to extend completely through the mat thickness.

A single application of bending moment sufficient to crack the mat from the top surface down and to the small observed crack width would not of itself, produce as deep a crack as has been observed. Mechanisms exist, however, which in combination with flexural strains, can produce deep, narrow cracks. One such mechanism is the combination of flexural and thermal strains. The mat, a placement of concrete of substantial volume, will experience considerable temperature increase in the middle due to hydration of cement followed by cooldown over a lengthy period of time. This thermal cycle can result in substantial (on the order of several hundred psi) concrete tensile stresses in the middle and compression stresses at the top and bottom. These stresses in combination with flexural stresses can create a narrow crack extending to substantial depth.

During the early stages of construction the mat experienced time-varying relative displacements; i.e., time-varying flexural curvatures. As shown by Figure 2, flexural curvature of the sense that is associated with tensile strain at the top of the mat was of a larger magnitude at an earlier time than when the cracks were first observed and measured. Corresponding to these earlier larger mat curvatures, there may have been larger crack widths than have been measured at any time since the cracks were first discovered. Presently observed crack depths may reflect these possible earlier crack widths. As construction continued, the mat relative deflections changed, decreasing the curvature and tending to close the cracks.

If, as reasoned above, crack widths at the top of the mat were larger at an earlier time, present crack widths serve only to indicate the maximum possible value of the present rebar tensile stress. If earlier crack width and associated rebar tensile stresses were substantially larger, and particularly if any rebar tensile yield strain was experienced, the present actual tensile stress must be less than implied by the present modest crack width and as estimated in Appendix 1.

There is no reliable basis for determining what actual maximum values of crack widths and associated rebar strain may have occurred during early stages of the mat construction. Different mechanisms have been identified which could account for the presently observed very modest crack widths together with substantial crack depths. A mechanism involving thermal strains can explain the presently observed condition without postulating earlier crack widths wider than at present. The other mechanism involves only flexure and postulates larger crack widths at an earlier time in the construction sequence. The actual sequence of events probably involves both of these mechanisms but the stress/strain conditions during construction are of no consequence to the safety of the structure in its completed state.

The validity of the construction process, including the mat displacement monitoring program, is evidenced by the completed structure not by crack widths and associated rebar stresses during the early construction stages. The earlier conditions are not relevant to the structural integrity of the completed structure, but they serve to explain, qualitatively, the depth of cracking.

5.3 WALL CRACKS

The cracks in RCB walls are found to be superficial by NDT and, therefore, appear to be caused by shrinkage. These cracks are apparently not related to adjacent basemat cracks, which were caused by mat flexure.

6.0 SIGNIFICANCE OF CRACKS AND EFFECTS ON STRUCTURAL INTEGRITY

The following conclusions are of importance in the determination of the significance of the cracks in the Waterford 3 basemat and their effect upon the structural integrity of the basemat:

1. The cracks are flexural cracks probably influenced in some cases with thermal strains. The consistent vertical orientation of the cracks is the evidence of this.

2. There are no inclined cracks within the basemat. This provides evidence that no excessive diagonal tension, hence no excessive shear, exists or has existed within the basemat.

3. There are no through cracks from top to bottom of the basemat with the possible exception of a very few localized areas. The cracks are primarily extending down from the top surface of the basemat. This is evidence that the cracks are primarily the result of flexure and that the flexure was of an upward convex nature which agrees with the observed deformations of the basemat during construction.

4. Presently there is virtually no water seepage or wetness present at any of the observed cracks and the amount of water seepage in the past has been minimal causing only a wetness of the basemat in the immediate vicinity of the cracks. The cracks are believed to have filled with a laitance derived from the parent concrete material. The general stress condition at the top of the basemat has become compression since the occurrence of the original cracking. This condition will not change during normal operation, hence, the continued minimal water seepage condition during the operation of the plant is assured. Therefore, the amount of water seepage presently meets, and will continue to meet, the original design intent for minimal water leakage.

5. The width of the cracks indicates a low present rebar stress (Appendix 1).

6. The crack pattern is predominantly in an east-west direction (Figure 1), localized in a band running east-west and centered near the RCB centerline. This band is within the region subjected to

the most extreme convex curvature during the early stages of construction (Figure 2). This evidence indicates that the cracks resulted from early settlements of the basemat occurring during placement or shortly thereafter. The cracks lying in a northeasterly or northwesterly direction were influenced by the rigidity of the early placements of the RCB wall.

7. The cracks in the RCB wall are shallow, shrinkage induced and are not related to the cracks in the basemat. The existence of cracks in the basemat and the wall at the same, or nearly the same, location appears to be coincidence.

8. The concrete quality is uniform and there are no significant voids and/or honeycombs within the mat. This indicates that the concrete consolidation was more than adequate during construction. The concrete strength is indicated to be 5,000 to 7,000 psi by NDT, which is higher than the required design strength of 4,000 psi and which is consistent with the strengths measured during the construction inspections.

FLEXURAL CONSIDERATIONS

"It is well known that load-induced tensile stresses result in cracks in concrete members. This point is readily acknowledged and accepted in concrete design. Current design procedures.... use reinforcing steel, not only to carry the tensile forces, but to obtain an adequate crack distribution and a reasonable limit on crack width."(1)

The cracks in the Waterford 3 foundation basemat are to be expected considering the flexural situation. They have no negative effect on the structural integrity or strength of the basemat or on the ability

---

(1) Causes, Evaluation, and Repair of Cracks in Concrete Structures - ACI 224 ACI Journal - May-June 1984, Paragraph 1.3.9.

of the basemat to resist adequately any design load combinations, nor can they significantly alter the design response of the structure to seismic vibrations. The cracks, being quite narrow and tight, will not increase the flexure of the basemat and hence will not cause any additional transfer of load to building members than that already accounted for in the design.

Reinforced concrete members subjected to flexural loads are designed to accept cracking of the concrete in the tension zone. The ACI code for design of reinforced concrete structures states that "tensile strength of concrete is to be neglected in flexural calculations,"[(2)] and that all tensile stresses are to be directed to the steel reinforcing. This is normal concrete cracked section analysis and the concrete must crack since it has a low tensile strain at fracture. Therefore, the steel is the structural component in the cracked tension zone.

When reversal of stresses occur and a previously cracked tension zone becomes subjected to compressive forces, the cracks close and the adjacent sides of the cracks bear against each other. The concrete crack surfaces in the Waterford 3 basemat are well able to bear against each other since they are tight and have been filled with laitance and under flexural loading the basemat will react the same as a normal concrete cracked section. Therefore, the flexural strength has experienced no degradation for bending in either direction and no significant increase in the flexure of the basemat will occur.

SHEAR CONSIDERATIONS

"If a (vertical) plane under consideration is an existing crack or interface, failure usually involves slippage or relative movement along

---

(2) Building Code Requirements for Reinforced Concrete, ACI 318-63, Paragraph 1503(e).

the crack or plane."[3] "If an initially cracked specimen is tested, shear can be transmitted only if lateral confinement or transverse steel exists. The irregularities of the surfaces of the two sides of the crack ride up on each other and this tends to open the crack and create forces in the transverse steel ...... In a heavily reinforced shear plane or one subjected to a normal compressive stress, the shear resistance due to friction and dowel action may reach the shear corresponding to failure of an initially uncracked specimen having the same characteristics. In such a case the crack locks and the behavior and strength are similar to those for an initially uncracked section."[4]

The Waterford basemat vertical cracks are both heavily reinforced and under "compressive stress."[5] In addition they are very narrow, do not extend through the basemat, and are filled with laitance. Essentially they are "locked." In actuality, they resemble construction joints and respond similarly.

<u>The Potential for "Shear Slip" on Mat Crack Planes</u>

If vertical shear on the basemat crack planes could produce "shear slip" (ie, a step change in vertical deflection across the crack plane), and if such shear slip were large, it would be appropriate to

---

(3) The Shear Strength of Reinforced Members - ACI-ASCE 426R-74, ACI Manual of Concrete Practice, 1983, Part 4, Paragraph 2.2.2.

(4) Ibid - Paragraph 2.2.2b.

(5) Review of Waterford 3 Basemat Analysis Structural Analysis Division, Dept. of Nuclear Energy, Brookhaven National Laboratory, July 18, 1984, p. 21.

investigate its possible significance to the dynamic response of the structure. For the reasons discussed below there is no basis for believing that slip will occur.

Background Regarding Shear Strength and Shear Slip on Crack Planes

The matter of shear strength along a crack plane, or a potential crack plane, has been relevant to reinforced concrete design. This is of interest primarily at the junctions of precast concrete members (where large shear forces must be transferred across such planes), in short reinforced concrete (R/C) brackets (where large shear forces sometimes accompanied by tensile forces must be transmitted across such planes), and in R/C membranes subjected to concurrent large shear and tensile forces acting on transverse crack planes. In contrast, for beams and slabs designed to resist internal transverse shear force and bending moments rather than membrane forces, the question of shear strength across potential transverse crack planes normally does not arise. Also, the evaluation of shear resistance across these planes is not normally a part of the design process. This is true even though transverse (flexural) cracks can develop in beams and slabs, particularly when there are bending moment reversals. It may be noted that provisions for shear reinforcement focus on inclined crack planes. The requirements for such reinforcement may be satisfied by transverse bars (which do not cross any potential transverse crack) and such a reinforcing pattern is acceptable for very substantial magnitudes of transverse shear stress. The validity of this practice for conventional beams and slabs reflects (a) the absence of large tension forces on actual or potential crack planes, which could imply large crack widths; and (b) the great shear strength and slip resistance along a crack plane if the crack is closed (or of small initial width), and if "clamping" (compression) force of adequate magnitude is available. This compression force may be provided either by the compression component of a bending moment acting on the section, by tension (flexural) steel crossing the section, by both, or by an externally applied compression force.

Much of the present understanding of shear strength and slip on crack planes was developed by research studies stimulated by the design of R/C containment shells for nuclear power plants. Such shells are subjected to very large membrane forces (i.e., large tension and shear forces) acting on transverse crack planes. The tensile forces can cause cracks of substantial width, and both shear strength and shear slip are matters of design interest. This is a very different condition than exists in the Waterford 3 basemat, but some of the results of the research on the membrane problem are ralevant to this discussion of the basemat. In particular, we refer to a report of tests conducted at Cornell University (Reference 3), which for crack planes with initial crack widths of 0.01 in., and subjected to cycles of shear stress reversals of about $\pm$ 180 psi, demonstrated the following results:

1) clamping forces developed in the bars that were used to restrain crack width growth did not exceed 20 percent of the applied shear force; and

2) total slip, after 25 cycles of shear reversal, did not exceed 0.01 in.

It should be noted that the clamping forces developed here were from reinforcing steel responding to the shear slip displacement, an active clamping force only present when slip occurs.

Basemat Strength and Slip Resistance on Crack Planes

The cracks in the basemat are predominantly east-west oriented, and are everywhere less than 0.01 inch in width. Of major importance is the fact that the crack planes are not subjected to any tensile force. Indeed there is a very substantial compression force (exerted by soil and water pressure on the north and south boundaries of the mat and the walls above), which is conservatively neglected for purposes of computing shear strength on the crack plane. With regard to its influence on slip, the effect of this compression force, conservatively ignored for strength, is particularly relevant and will be accounted for. Any north-south bending moment, whether positive or negative, which may be acting on the crack plane does not diminish the shear strength of the crack plane. Bending moment which causes tension force in the bottom rebars must cause an equal and opposite compression force in the top few feet of the section. Similarly, bending moment which causes tension force in the top rebars must cause an equal and opposite compression force in the bottom few feet of the section. Thus, diminished resistance in the bottom (or top) is offset by an enhanced resistance in the top (or bottom).

In the regions of interest the top rebars are #11 @ 6", i.e., 3.12 in^2/ft, and the minimum bottom rebars are #11 @ 6" + #11 @ 12", i.e., 4.68 in^2/ft. Over a representative crack plane length (50 ft) the maximum total shear forces on any crack plane are found at either end of the East-West running cracks. The maximum total shear forces on these 50 ft representative lengths correspond to the following values:

Loading Condition	Total Shear Force	Unit Shear Force
1.5 x Gravity Load	42 K/ft	27 psi
1.1 x E-W EQ*	96 K/ft	61 psi
1.1 x Vert EQ	5 K/ft	3 psi
1.1 (Vert EQ + E-W EQ)	101 K/ft	64 psi
1.5 Gravity + 1.1 (Vert EQ + E-W EQ)	143 K/ft	91 psi

*N-S EQ (earthquake) gives smaller shear forces.

It should be noted that averaging of forces over a 50 ft crack length is very conservative since this is only about 4 times the mat thickness. The average shear forces would decrease rapidly with increase in the crack length considered. It also should be noted that the corresponding shear forces on any other 50 ft length of any other cracks are less than the values tabulated above.

Shear Capacities

Using shear provisions of Section 11.7.4, ACI-1983, shear strength of the entire section is given by:

$$V = \Phi V_n = \Phi A_{vf} f_y \mu$$

where V = available shear strength at section

Φ = strength reduction factor = 0.85

V_n = nominal shear strength

A_{vf} = area of shear-friction reinforcement

f_y = specified yield strength of reinforcement = 60 ksi

μ = coefficient of friction = 1.4 λ

λ = correction factor related to unit weight of concrete = 1.0

therefore,

$$V = 0.85\ (3.12 + 4.68)\ 60 \times 1.4 \times 1.0 = 556.9\ \text{K/ft}$$

which corresponds to an average unit shear strength of:

$$v = \frac{556,900}{12 \times 11 \times 12} = 352\ \text{psi}$$

Because the rebars are concentrated near the top and bottom of the section, rather than distributed throughout the depth of the section we conservatively reduce the above shear capacity by 50 percent, i.e., to 278 K/ft. This is 1.9 times the 143 K/ft shear demand.

It is clear that the shear strength along the crack plane, even ignoring the inescapable active compression force, is much in excess of the demand.

Slip Resistance

As reported in Reference 3, for an initial crack width of 0.01 inches, and cycles of shear stress reversal to 180 psi a slip of about 0.004 in. was developed at the end of the first cycle increasing to 0.01 in. after 25 cycles. Moreover the maximum clamping force developed during this cycling was only 20 percent of the applied shear force. In the mat we are interested in an applied shear stress of 91 psi, for which a 20 percent clamping force would be 18 psi.

The compression acting on the cracked section, due to horizontal soil and water pressure on the mat and walls, is 50 psi. Based on the finite element model, this compression exists in all areas of the basemat during earthquake loading conditions with the small exception of a very narrow band immediately adjacent to the north and south walls. It is not credible that this compression stress, reduced as may be reasonable for the effect of an earthquake, would not still be substantially in excess of 18 psi. This means that more than the required clamping pressure of 18 psi is available from the outset; i.e., no rebar tension is required to provide the required clamping force. Since, the clamping force is a passive force, the friction resulting from it is available without shear slip and is a static friction.

The conclusion that is drawn that the shear resistance across the crack is a state of static friction wherein the available static friction must be overcome prior to the occurance of any shear slip. Since the available friction is at least equal to and undoubtedly far in excess of the applied shear stress we conclude that the shear resistance would develop without any significant slip. Therefore, there is no change in the rigidity of the mat and no effect upon the dynamic response of the basemat to the earthquake.

7.0 CONCLUSION

Considering each of the above items individually and in concert, we conclude that the cracks in the Waterford 3 basemat, as defined by the nondestructive testing, have no adverse influence on the structural integrity of the basemat. It is fully capable of functioning as required by the design in accordance with the pertinent codes.

REFERENCES

1. Affidavit of Joseph L Ehasz, Ebasco Services Incorporated, submitted before the Atomic Safety and Licensing Appeal Board, USNRC, September 1983.

2. "NPIS Wall Hairline Crack Evaluation," by Ebasco Services Incorporated, April 1984.

3. J P Laible, R N White, and P Gergely, "Experimental Investigation of Seismic Shear Transfer Across Cracks in Concrete Nuclear Containment Vessels," ACI SP 53-9, Reinforced Concrete Structures in Seismic Zones, 1977.

TABLE 1 - SUMMARY OF CRACKS WEST SIDE OF RCB

Family	Crack I.D.	Test Lines	Length (exposed)	Top Crack Depth (ft.) Min	Max	Average	Family Spacing	Presence of Subsurface Cracks (See Notes): Bottom Crack, Below Bottom Re-bar	Bottom Crack, Through Bottom Re-bar	Middle Crack	In
I	A	7	7'- 6	1	2	2		*	*	*	v
	B	7	9'- 0	2	3	3		*	*	*	v
	C	12	16'- 6	1	3	2		*	*	*	v
							±10'	*	*	*	v
II	D	5	6'- 0	2	5	4		*	***	*	v
	E	1	2'- 0	3	3	3		*	*	**	v
	F	6	9'- 0	4	10	5		**	**	*	v
	G	4	6'- 0	1	5	4		*	*	*	v
							±16'				
III	I	4	5'- 0	7	10	8		**	**	*	v
	H	6	9'- 0	5	10	8		**	**	*	v
	J	20	28'- 0	3	12	9		***	****	**	v
	K	10	13'- 0	3	11	8		**	***	*	v
							±10'				
IV	L	10	28'- 0	6	10	8		**	**	*	v
							±8'				

Notes: *None

**Presence of crack is not probable since only at one or two test line location(s).

***Presence of crack is probable since indication at several test locations but not interconnected with top cr

****Similar to *** except probably interconnected with top crack.

(Sheet 1 of 2)

TABLE 1 - SUMMARY OF CRACKS WEST SIDE OF RCB (Cont'd)

Family	Crack I.D.	Top Crack: Test Lines	Top Crack: Length (exposed)	Top Crack: Depth (ft.) Min	Top Crack: Depth (ft.) Max	Top Crack: Depth (ft.) Average	Family Spacing	Presence of Subsurface Cracks (See Notes): Bottom Crack: Below Bottom Re-bar	Presence of Subsurface Cracks (See Notes): Bottom Crack: Through Bottom Re-bar	Presence of Subsurface Cracks (See Notes): Middle Crack	Inclinati
V	M	4	6'- 0	4	5	4		*	*	*	vertical
	N	3	5'- 0	2	6	3		*	*	*	vertical
	2	3	5'- 0	1	3	2		*	*	*	vertical
	3	9	12'- 0	1	5	2		*	*	*	vertical
	P	9	14'- 0	8	10	9		*	**	*	vertical
	R	1	2'- 0	2	2	2		*	*	*	vertical
	Q	3	8'- 0	3	5	4		*	*	*	vertical
	S	3	4'- 0	4	4	4		*	*	*	vertical
	T	14	20'- 0	3	10	6		*	***	*	vertical
	Y	3	6'- 0	1	1	1		*	*	*	vertical
							± 6'				
VI	U	9	14'- 0	2	10	5		*	**	*	vertical
	V	5	13'- 0	2	5	3		*	*	*	vertical
	X	22	25'- 0(+)	1	5	3		*	*	*	vertical
VII	West Diagonal	19	27'- 0	1	4	3		**	***	*	vertical

Notes: *None
**Presence of crack is not probable since only at one or two test line location(s).
***Presence of crack is probable since indication at several test locations but not interconnected with top crack.
****Similar to *** except probably interconnected with top crack.

TABLE 2 - SUMMARY OF CRACKS EAST SIDE OF RCB

Family	Crack I.D.	Test Lines	Length (exposed)	Top Crack Depth (ft.) Min	Max	Average	Family Spacing	Presence of Subsurface Cracks (See Notes): Bottom Crack Below Bottom Re-bar	Bottom Crack Through Bottom Re-bar	Middle Crack	In
Ie	Ae	4	6'- 0	1	1	1		*	*	*	V
	Be-Ce	5	6'- 0	1	4	3		*	*	*	V
	De	2	4'- 9	1	1	1		*	*	*	V
	le	2	3'- 0	3	3	3		*	*	*	V
							±10'				
IIe	Ee	4	4'- 6	1	1	1		*	*	*	V
	Fe	8	12'- 0	2	10	6		*	***	*	V
							+13'				
IIIe	He	5	6'- 0	2	3	2		**	*	**	V
	Je	5	7'- 0	2	4	3		***	*	**	V
	Le	8	13'- 0	3	12	7		***	**	*	V
							±11'				
IVe	Ke	15	26'- 0	4	12	8		**	****	*	V
							±16'				
Ve	De1	3	4'- 0	1	1	1		*	*	*	Ve
	De3	15	23'- 0	1	6	3		*	*	*	Ve
	De4	5	10'- 0	1	1	1		*	*	**	Ve
							±15'				

Notes: *None
**Presence of crack is not probable since only at one or two test line location(s).
***Presence of crack is probable since indication at several test locations but not interconnected with top cra
****Similar to *** except probably interconnected with top crack.

TABLE 2 - SUMMARY OF CRACKS EAST SIDE OF RCB (Cont'd)

Family	Crack I.D.	Top Crack						Family Spacing	Presence of Subsurface Cracks (See Notes)			
		Test Lines	Length (exposed)	Depth (ft.)					Bottom Crack		Middle Crack	Inc
				Min	Max	Average			Below Bottom Re-bar	Through Bottom Re-bar		
VIe	De5	17	24'-0	1	10	3			***	*	***	ve
	De6	5	7'-3	2	6	4			**	*	*	ve
								± 15'				
VIIe	De7	9	12'- 0	1	6	3			*	**	***	ve
	De8	8	10'- 0	1	3	2			*	***	***	ve
	De9	11	15'- 0	1	5	2			**	*	***	ve

Notes: *None
**Presence of crack is not probable since only at one or two test line location(s).
***Presence of crack is probable since indication at several test locations but not interconnected with top cra
****Similar to *** except probably interconnected with top crack.

TABLE 3 - SUMMARY OF CRACKS BENEATH RCB

Crack I.D.	Correlation with 1977 Mapping	Depth	Inclination	Spacing @ C.L. RCB
6	None (Note 1)	Variable	Vertical	
				18'
2	None (Note 1)	"	"	
				12'
1	Yes	"	"	
				9'
7	Partial	"	"	
				6'
3	Yes	"	"	
				9'
5	Partial	"	"	
				13'
4	Yes	"	"	
			Average Spacing =	11'

Note 1 - This crack was not identified during 1977 mapping of cracks beneath RCB.

TABLE 4 - SUMMARY OF CRACKS IN RCB WALLS

Crack I.D.	Test Lines	Maximum Dept of Penetration (ft.)	Inclination	Remarks
RCB 1	3	1	Perpendicular to wall surface	Wall thickness = 10
RCB 2	3	1	Perpendicular to wall surface	Wall thickness = 10
RCB 3	3	1	Perpendicular to wall surface	Wall thickness = 10
RCB 4	3	1	Perpendicular to wall surface	Wall thickness = 10

APPENDIX 1

REINFORCING STEEL STRESS AS DEFINED BY CRACK WIDTH

Gergely & Lutz Equation ("Causes, Evaluation and Repair of Cracks in Concrete," ACI 224, ACI Journal May-June 1984, p. 218).

$$\omega = 0.076\ \beta\ f_s \sqrt[3]{d_c A_1} \times 10^{-3}$$

$$A_1 = 6 \times 8.5 = 51 \text{ in}^2$$

$$\beta = \frac{10.5}{10.125} = 1.04$$

$$d_c = 4.25 \text{ in}$$

ω = 5 mils (crack width)

f_s = 10,500 psi = 10.5 ksi

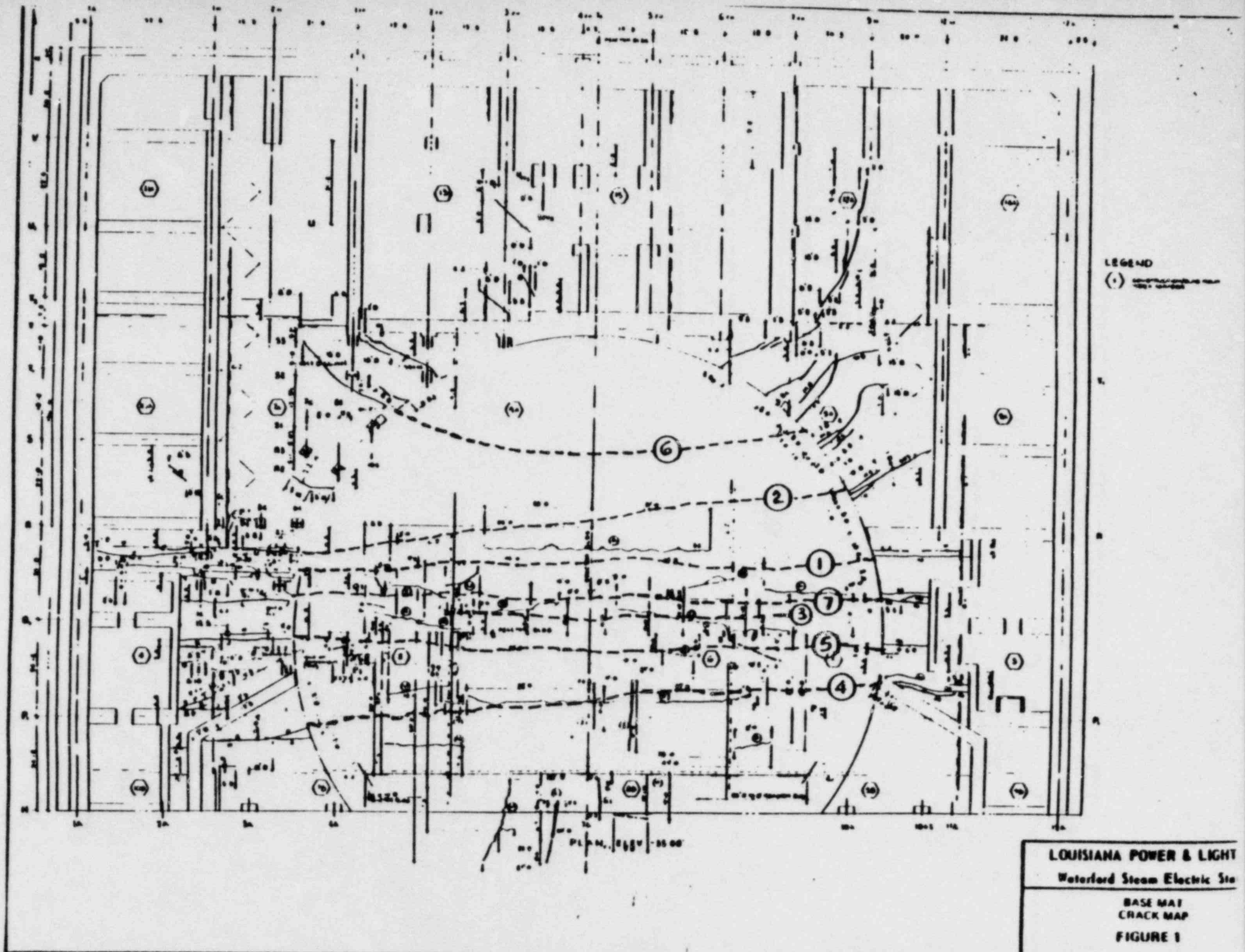

LOUISIANA POWER & LIGHT
Waterford Steam Electric Sta

BASE MAT
CRACK MAP

FIGURE 1

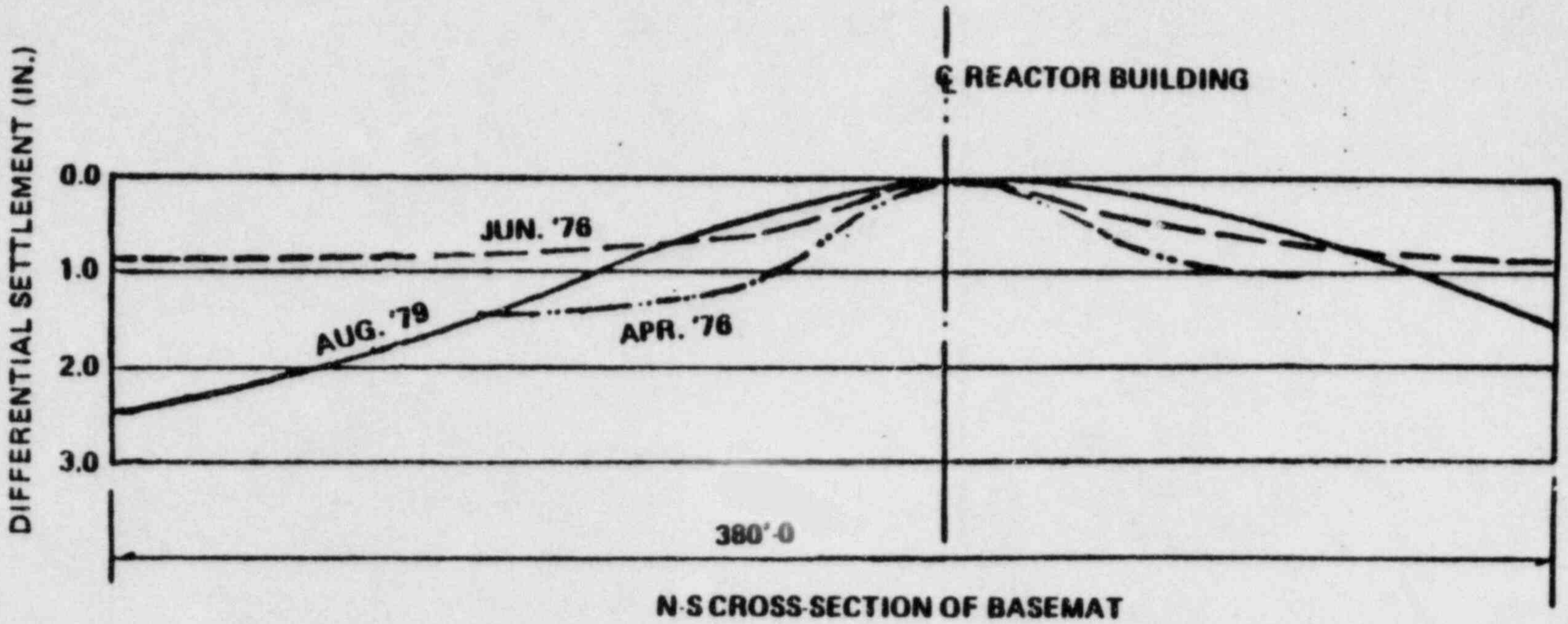

NOTES:

VERTICAL EXAGGERATION = 300

DIFFERENTIAL SETTLEMENT IS FROM DAY OF PLACING AND INCLUDES SETTLEMENTS AT VERY EARLY AGES OF EACH CONCRETE PLACEMENT

LOUISIANA POWER & LIGHT CO.
Waterford Steam Electric Station

BASEMAT CURVATURE

Figure 2

the extruded concrete. The machine is unlocked from the strand at a joint and locked on to strands at the beginning of the next slab.

8. Tiebars are depressed into the concrete with a wheel type device and a plastic parting strip installed to form a longitudinal joint. After the finishing machine passes, metal caps are placed on the top of the I-beam and the angle to build them up to the 6 in. pavement thickness. The adjacent concrete is hand finished and curing applied.
9. The concrete is then allowed to gain strength. If the pavement is expected to shrink or contract it may be necessary to apply more than one step of post-tensioning to prevent tensile cracks from occurring. If the concrete remains at close to its placement temperature for several days it is possible to apply full post-tensioning when the concrete reaches 3000 psi compressive strength (2 to 3 days).
10. A gang of four jacks with 10-in. throw is lowered from a mobile cart into the blockouts at the end of a slab and a jack is positioned on the end of each strand in one lane. Each strand is then pulled to 40 kips. Since this load will elongate the strand approximately 40 in. in a 500 ft. slab, the jacks would have to be regripped several times. The gang would then be moved to the adjacent lane and that completed. Next the jacks are moved to the other end of the slab and the strands are pulled just a few inches to bring that end to full force since about 20 percent of the force from the other end was lost due to friction. The adjacent lane is also done and the jacks moved to start on a new slab.
11. With the stressing completed, the 24 ft. long angle is removed. A second I-beam 6 in. high is fitted into place adjacent to the one already there and connected via dowels. Extension rods are connected to the strand chucks which are exposed on the opposite side where the angle used to be. The 3-ft. length of blockout is then concreted and after it gains adequate strength is post-tensioned against the main slab with torque nuts on the ends of the extension rods.
12. After the blockouts are filled and post-tensioned only one small opening between the two I-beams is all that remains to accommodate length changes of the slabs. Foamed-in-place polyurethane is used to fill the opening.

Overall a very efficient operation can be effected. The two major areas of concern are getting well consolidated concrete at the joints and in determining the time for tensioning. The tensioning operation is relatively simple and poses no problems. Filling the gaps with concrete will require some care but it should be fairly simple since each requires only about 1½ cu. yd. of concrete.

Other agencies are encouraged to place additional slabs in order to improve paving techniques and to develop additional design criteria. The FHWA is developing specifications for constructing additional sections and these will be available upon request.

Discussion of this paper is invited. Please forward your discussion to PCI Headquarters by July 1 to permit publication in the July-August 1972 issue of the PCI JOURNAL.

SHEAR TRANSFER IN REINFORCED CONCRETE—RECENT RESEARCH

Alan H. Mattock
University of Washington
Seattle, Washington

Neil M. Hawkins
University of Washington
Seattle, Washington

Shows how concrete strength, shear plane characteristics, reinforcement, and direct stress affect the shear transfer strength of reinforced concrete. Fundamental behavior of test specimens under load is reported, and hypotheses to explain the behavior are developed. It is concluded that shear-friction provisions of ACI 318-71 give a conservative estimate of shear-transfer strength below the stated limit of 800 psi. A design equation to develop higher shear transfer strength is presented.

Test program

Shear transfer across a definite plane must frequently be considered in the design of precast concrete connections[1,2]. A continuing study of the factors affecting shear transfer strength is in progress at the University of Washington. Factors so far included in the study are as follows:

1. The characteristics of the shear plane
2. The characteristics of the reinforcement
3. The concrete strength
4. Direct stresses acting parallel and transverse to the shear plane.

The influence of the first three factors has been studied in tests[3] of monolithically cast "push-off" specimens as seen in Fig. 1(a). Tests[4,5] to study the influence of direct stresses acting parallel and transverse to the shear plane were made on the "pull-off" and modified push-off specimens shown in Figs. 1(b) and 1(c) respectively. In all cases, the shear transfer reinforcement crosses the shear plane at right angles and is securely anchored so that it can develop its yield strength in tension.

ATTACHMENT 2

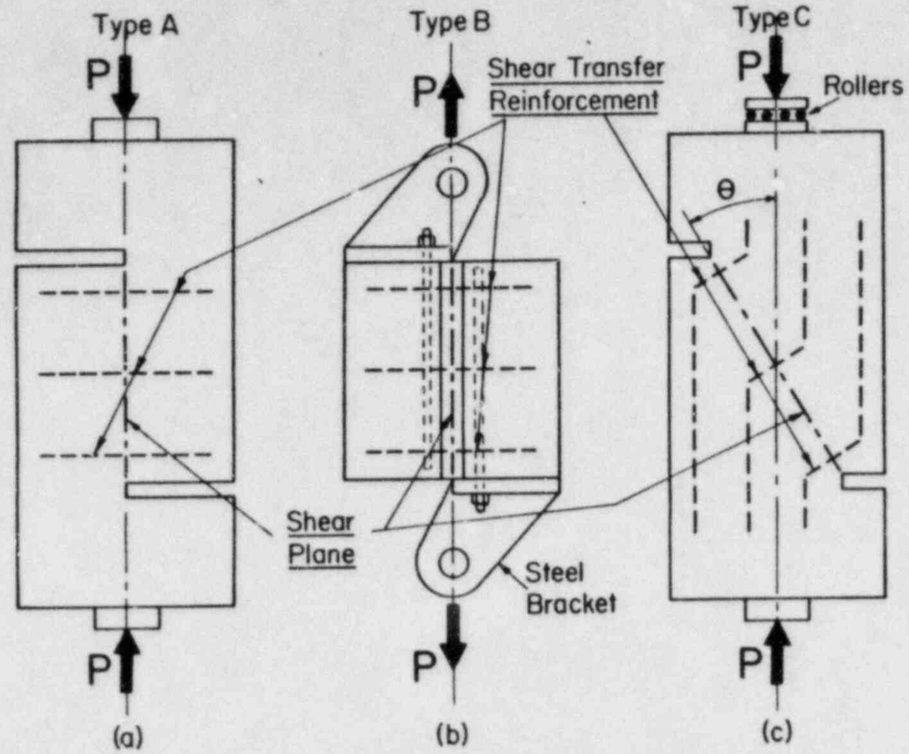

Fig. 1. Shear transfer test specimens: (a) push-off; (b) pull-off; (c) modified push-off

Additional reinforcement is provided away from the shear plane, to prevent failures other than along the shear plane. The length and width of the shear planes were 10 x 5 in., 12 x 4¾ in., and 12 x 6 in. (approx. 25 x 13 cm, 30 x 12 cm, and 30 x 15 cm) in the push-off, pull-off and modified push-off specimens respectively. When loaded concentrically by a force P, the shear along the shear plane is equal to P in the push-off and pull-off specimens. In the modified push-off specimens, the concentric force P produces a shear force $P \cos \theta$ along the shear plane and a compressive normal force $P \sin \theta$ across the shear plane. Six different values of θ were used to give different ratios of shear stress to transverse normal stress. The test program is summarized in Table 1.

The specimens were subjected to monotonic loading to failure. In all cases, slip along the shear plane was measured, and in some instances the lateral separation at the shear plane was also measured. Cracks were marked on the faces of the specimens as they developed. Detailed data for Series 1 to 6 have already been published[3]. The data for Series 7 to 10 are summarized in Tables 2 and 3. For convenience, the ultimate shear strengths are expressed as average shear stresses v_u, obtained by dividing the ultimate shear force V_u by the area of the shear plane bd (d is the length of the shear plane and b its width).

Table 1. Test program

Test series	Description	Specimen type	Number of tests
1	Push-off tests of initially uncracked specimens. Reinforcement size constant, spacing varies. $f'_c \approx 4000$ psi, $f_y \approx 50$ ksi.	A	13
2	Push-off tests of initially cracked specimens. Reinforcement size constant, spacing varies. $f'_c \approx 4000$ psi, $f_y \approx 50$ ksi.	A	6
3	Push-off tests of initially cracked specimens. Reinforcement size varies, spacing constant. $f'_c \approx 4000$ psi, $f_y \approx 50$ ksi.	A	5
4	Push-off tests of initially cracked specimens. Higher strength reinforcement, $f_y \approx 66$ ksi. Reinforcement size constant, spacing varies. $f'_c \approx 4000$ psi.	A	5
5	Push-off tests of initially cracked specimens. Low strength concrete, $f'_c \approx 2500$ psi. Reinforcement size constant, spacing varies. $f_y \approx 50$ ksi.	A	5
6	Push-off tests of both initially cracked and uncracked specimens. Dowel action destroyed by short rubber sleeves on reinforcement across shear plane. $f'_c \approx 4000$ psi, $f_y \approx 50$ ksi.	A	4
7	Pull-off tests of initially uncracked specimens. Reinforcement size and spacing varies. $f'_c \approx 5000$ psi, $f_y \approx 50$ ksi.	B	6
8	Pull-off tests of initially cracked specimens. Reinforcement size and spacing varies. $f'_c \approx 5000$ psi, $f_y \approx 50$ ksi.	B	6
9	Modified push-off tests of initially uncracked specimens. Reinforcement size constant, spacing varies. Angle θ varies (0, 15°, 30°, 45°). $f'_c \approx 5500$ psi, $f_y \approx 52$ ksi.	C	6
10	Modified push-off tests of initially cracked specimens. Reinforcement size constant, spacing varies. Angle θ varies (0, 15°, 30°, 45°, 60°, 75°). $f'_c \approx 4000$ and 6000 psi, $f_y \approx 52$ ksi.	C	10

Table 2. Test data, Series 7 and 8

Specimen number*	Reinforcement bar size	Number of stirrups (2 legs each)	Reinforcement yield point, f_y, ksi	Concrete strength, f'_c, psi	pf_y, psi	v_u, psi
7.1	#3	2	49.5	4850	384	851
7.2	#3	3	49.5	5120	576	908
7.3	#3	4	49.5	5050	768	974
7.4	#2	2	56.0	5410	193	567
7.5	#2	3	56.0	5070	289	609
7.6	#2	5	56.0	5100	481	846
8.1	#3	2	49.5	4850	384	697
8.2	#3	3	49.5	5120	576	888
8.3	#3	4	49.5	5050	768	925
8.4	#2	2	56.0	5410	193	521
8.5	#2	3	56.0	5070	289	572
8.6	#2	5	56.0	5100	481	746

*Specimens of Series 7 were initially uncracked; specimens of Series 8 were cracked along the shear plane before test.

Characteristics of the shear plane. Mast[2] pointed out the need to consider the case where a crack may exist along the shear plane before shear is applied. Such cracks occur for a variety of reasons unrelated to shear, such as tension forces caused by restrained shrinkage or temperature deformations or accidental dropping of a member. Certain shear transfer test specimens were therefore cracked along the shear plane by the application of transverse line loads, before application of shear loading.

Slip was measurable from the beginning of the shear test for the initially cracked specimens. However, no movement occurred in the initially uncracked Type A specimens until diagonal tension cracks became visible at shear stresses of from 500 to 700 psi (35–49 kgf/cm²). These cracks crossed the shear plane at an angle of from 40 to 50 deg. They were each about 2 in. (5 cm) long, spaced 1 to 2 in. (2½ to 5 cm) apart along the shear plane. After these cracks formed, there was a relative longitudinal movement of the two halves of the initially uncracked specimens. This was due to rotation of the short concrete struts formed by the diagonal tension cracks, when the shear transfer reinforcement stretched. It was found that if a crack exists in the shear plane before the application of shear, then the slip at all stages of loading is greater than when such a crack does not exist.

A crack in the shear plane reduces the ultimate shear strength of under-reinforced specimens (Fig. 2). The decrease is greater in the push-off specimens than in the pull-off specimens. The shear strength of the initially cracked specimens is not directly proportional to the amount of reinforcement. Because of the observed weakening effect of a crack in the shear plane, most of the subsequent tests were made on initially cracked specimens, in order to obtain lower bound values of shear strength.

Table 3. Test data, Series 9 and 10

Specimen number[1]	Angle θ, deg.	Number of bars[2]	Reinforcement yield point, f_y, ksi	Concrete strength, f'_c, psi	pf_y, psi	σ_{Nx}, psi	$pf_y + \sigma_{Nx}$, psi	v_u, psi	Failure type[3]
9.1	45	10	52.4	5500	800	2460	3260	2460	S
9.2	30	12	52.2	5500	956	1480	2436	2560	S
9.3	15	12	52.3	3940	976	406	1382	1515	S
9.4	0	12	53.7	3940	985	0	985	1389	S
9.5	30	8	51.0	6440	623	1655	2278	2870	S
9.6	30	4	51.0	6440	312	1600	1912	2770	S
10.1	75	6	51.8	3450	475	3220	3695	862	C
10.2	75	6	52.0	4390	476	3920	4396	1049	C
10.3	60	8	51.8	3450	632	2780	3412	1610	C
10.4	60	8	53.0	4390	648	3060	3708	1770	C
10.5	45	10	52.7	4630	805	2265	3070	2265	S
10.6	30	12	52.0	4630	954	1250	2204	2165	S
10.7	15	12	52.4	4020	962	387	1349	1445	S
10.8	0	12	53.7	4020	985	0	985	1115	S
10.9	30	8	51.0	5800	623	1490	2113	2590	S
10.10	30	4	51.0	5800	312	813	1125	1410	S

1. Specimens of Series 9 were initially uncracked; specimens of Series 10 were cracked along the shear plane before test.
2. All reinforcing bars were No. 3's arranged in pairs crossing the shear plane.
3. S = shear; C = compression.

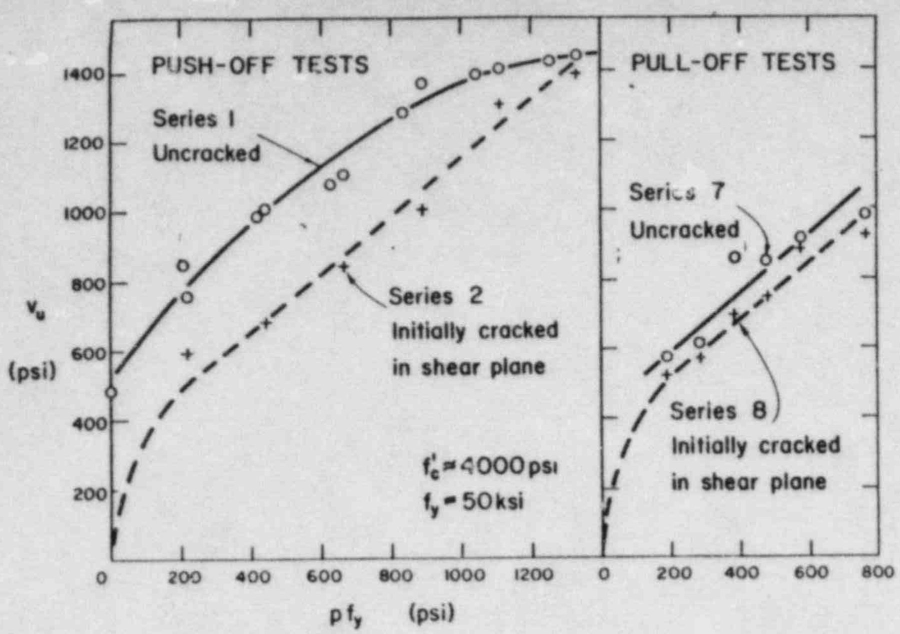

Fig. 2 Variation of shear transfer strength reinforcement parameter pf_y, with and without an initial crack along the shear plane

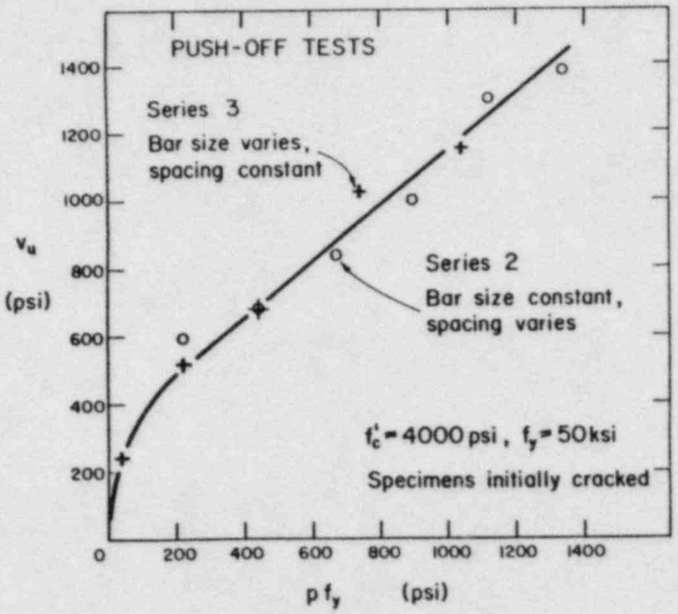

Fig. 3. Effect of stirrup bar size and spacing on the shear transfer strength of initially cracked push-off specimens

Characteristics of the reinforcement. The reinforcement parameter pf_y can be changed by varying either the reinforcement ratio p, the reinforcement yield strength f_y, or both. Also, for a given shear plane the reinforcement ratio can be changed by changing the bar size and/or the bar spacing. In Fig. 3, the results of tests of Series 2 and 3 are compared to determine whether the way in which the reinforcement ratio is changed has any effect on the relationship between ultimate shear strength and the reinforcement parameter pf_y. In Series 2, p was changed by varying the stirrup spacing, the bar size (No. 3) (9.5 mm) being constant. In Series 3, P was changed by varying the bar size between ⅛ in. diam. and No. 5 (3.2 and 15.9 mm) while maintaining a constant spacing of 5 in. (12.7 cm). Fig. 3 shows that the way in which p is changed does not affect the relationship between shear strength and the reinforcement parameter pf_y.

In the tests so far discussed the shear transfer reinforcement had a yield strength of about 50 ksi (3500 kgf/cm²). A group of push-off specimens was therefore tested in which the reinforcement had a yield strength of 66 ksi (4640 kgf/cm²), to check whether the relationship between v_u and pf_y was independent of f_y, and also to check whether it was possible to develop the yield strength of this higher strength steel. It was found that for given values of pf_y, the specimens with 66 ksi steel had slightly higher shear strengths than the specimens reinforced with the 50 ksi steel. This appears to indicate that at ultimate strength the higher strength steel stirrups developed a stress

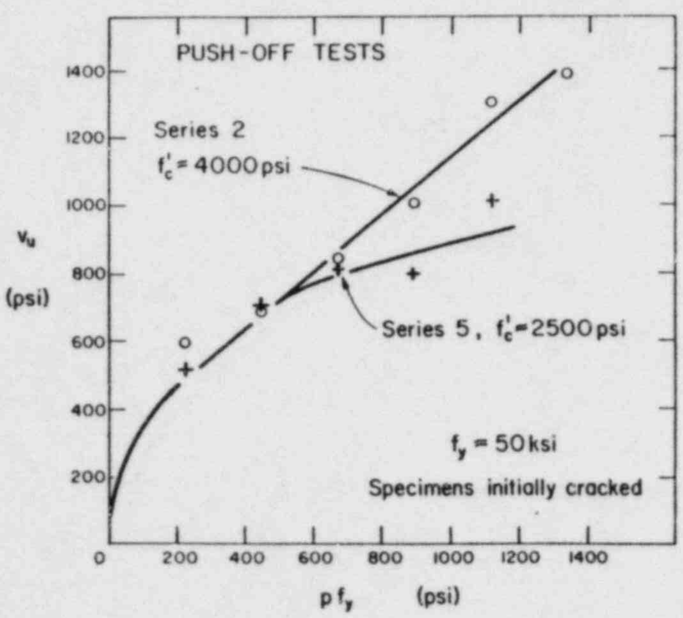

Fig. 4. Effect of concrete strength on the shear transfer strength of initially cracked push-off specimens

greater than their yield point, i.e., strain hardening had occurred. This is quite possible, as the yield plateau of the higher strength reinforcement was considerably shorter than that of the intermediate grade reinforcement. It therefore appears conservative to assume that the relationship between pf_y and v_u is the same for higher strength reinforcement as for intermediate grade reinforcement, provided the yield strength does not exceed 66 ksi.

Concrete strength. The effect of variation in concrete strength on the shear strength of initially cracked push-off specimens is illustrated in Fig. 4. The specimens of Series 2 and 5 were identical in all respects except for concrete strength, Series 2 having 4000 psi (281 kgf/cm²) concrete and Series 5 having 2500 psi (176 kgf/cm²) concrete. For values of pf_y below about 600 psi (42 kgf/cm²) the concrete strength does not appear to affect the shear transfer strength. For higher values of pf_y the shear strength is lower for the lower strength concrete. The concrete strength therefore appears to set an upper limit value of pf_y, below which the relationship between v_u and pf_y established for 4000 psi concrete would hold for any strength of concrete equal to or greater than the strength being considered, and above which the shear strength increases at a lesser rate for the concrete strength being considered. This change in behavior is discussed later.

Direct stress parallel to the shear plane. In an earlier report[3] a method was proposed for the calculation of the shear transfer strength of initially uncracked concrete. This was based on the average shear and normal stresses acting on a concrete element in the shear plane and made use of the failure envelope for concrete proposed by Zia.* This approach predicted the relationship between v_u and pf_y very closely for the tests of initially uncracked push-off specimens reported here, and also for tests of larger initially uncracked composite push-off specimens reported by Anderson[7]. In the push-off test, direct compressive stresses exist parallel to the shear plane, and these were taken into account in the calculation.

Using this method of calculation, an analytical study was made of the influence on shear transfer strength of direct stress parallel to the shear plane. From these calculations it appeared that if a direct tension stress existed parallel to the shear plane, then the shear transfer strength would increase more slowly, as pf_y was increased, than in the push-off test where a direct compressive stress exists parallel to the shear plane. This conclusion was disturbing from the designer's point of view, since in many practical situations there is a direct tensile stress parallel to the shear plane. It was therefore decided to study this problem with pull-off tests using specimens of the type shown in Fig. 1(b). The shear is applied to the shear plane by a concentric tension force acting on the specimen through steel brackets bolted to longitudinal reinforcing bars embedded in the specimen on either side of the shear plane. In these specimens a direct tension stress exists parallel to the shear plane, the average intensity of which is about half the intensity of the applied shear stress. In the push-off specimens tested previously, a direct compressive stress existed parallel to the shear plane, the average intensity of which was equal to that of the applied shear stress.

The ultimate shear strengths of the pull-off and push-off specimens are compared in Fig. 5. For initially uncracked specimens, the pull-off tests gave lower shear strengths than the push-off tests, indicating that a direct tension stress parallel to the shear plane

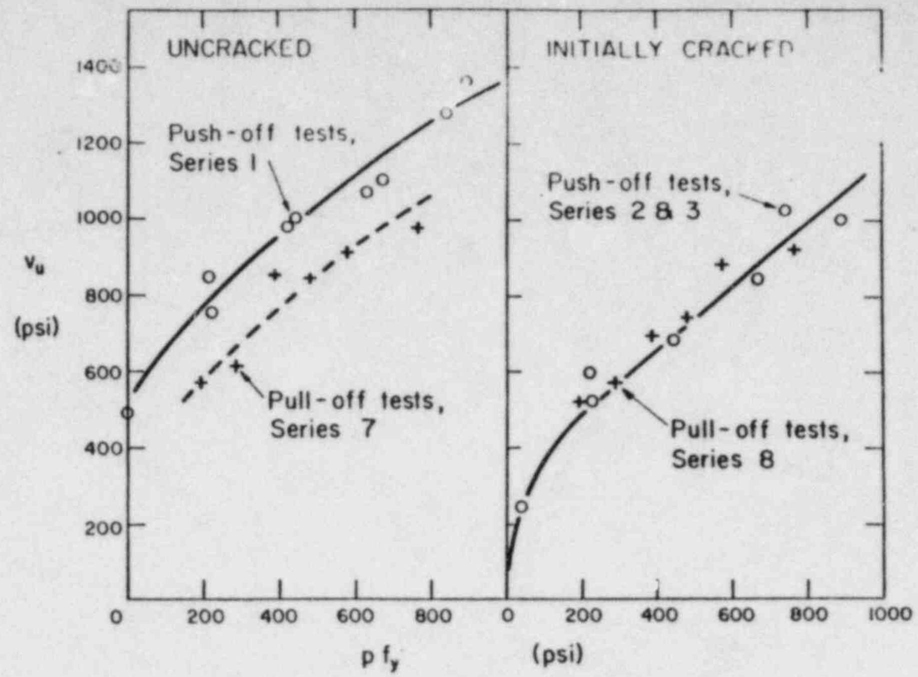

Fig. 5. Effect on shear transfer strength of direct stress acting parallel to the shear plane

is detrimental to shear transfer strength in initially uncracked concrete. However, the reduction in shear strength appears to be due to a reduction in the cohesion contribution of the concrete, and the rate of increase in v_u with increase in pf_y is approximately the same in both the pull-off and push-off tests. This indicates that the method of calculation proposed earlier[3] is faulty and cannot be extrapolated to the case of the pull-off test.

For specimens cracked along the shear plane before being loaded in shear, the shear strengths of the push-off and the pull-off specmiens are essentially the same for any given value of pf_y. This is important practically, since it indicates that direct stresses parallel to the shear plane may be ignored in design for shear transfer, if the design is based on the relationship between v_u and pf_y obtained in tests of initially cracked specimens.

Direct stress transverse to the shear plane. The effect of compressive stresses acting transverse to the shear plane was studied in Series 9 and 10. Modified push-off specimens were used, as shown in Fig. 1(c). The depth of the block-outs in the specimens was adjusted so that the length of the shear plane joining their ends remained constant as the angle θ varied. A system of rollers on the top of the specimen permitted separations to develop, even for relatively large applied loads. The spec-

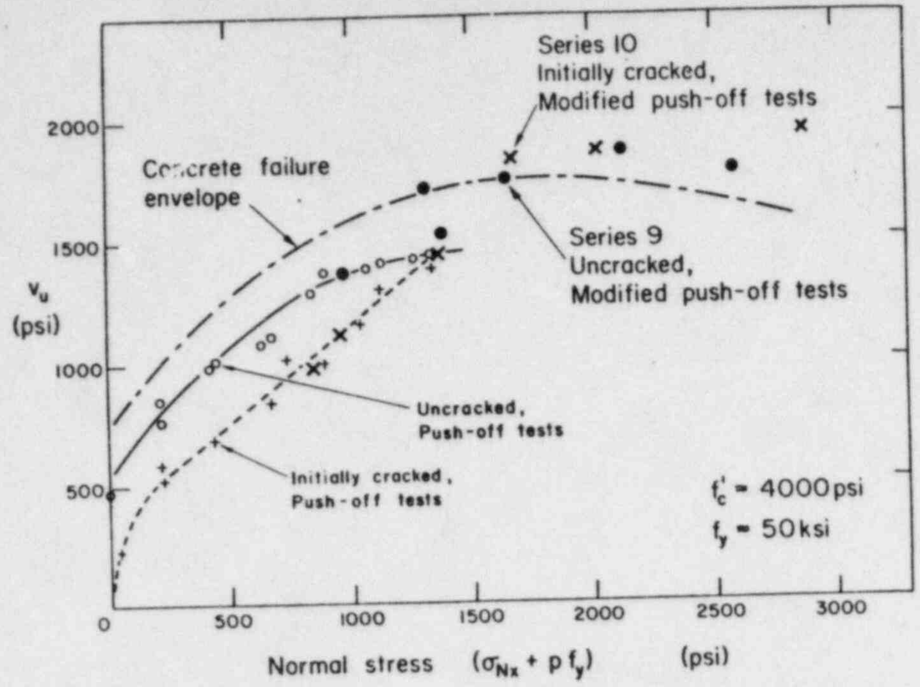

Fig. 6. Effect on shear transfer strength of direct stress acting transverse to the shear plane

imens of Series 10 were initially cracked along the shear plane, while those of Series 9 were initially uncracked.

Failures were characterized by a shearing action along the shear plane when angle θ was 45 deg. or less, and by a crushing failure across the plane for θ of 60 or 75 deg. The deformations of the initially uncracked specimens were extremely small until diagonal tension cracks developed across the shear plane at about 60 to 70 percent of the ultimate strength. As in the push-off specimens, these cracks formed at an angle of about 45 deg. to the shear plane. They were about 2 in. (5 cm) long, and between 1 and 2 in. (2½ to 5 cm) apart. In specimens with angle θ of 30 deg. or less, failure occurred with a continuous crack propagating through the diagonal tension cracks, along the shear plane. Deformations developed rapidly after diagonal tension cracking, at a rate which increased continuously with increasing load, but decreased as θ increased. The slips at failure were in excess of 0.03 in. (0.76 mm) and the separations were large enough to indicate yielding of the reinforcement when θ was 30 deg. or less. For the specimens with θ equal to 45 deg., separations did not develop rapidly until immediately prior to failure. For the specimens with θ of 30 deg. and having differing values of pf_y, the load-slip relationships were not influenced by the value of pf_y until immediately prior to failure.

Significant deformations of the precracked specimens occurred from the commencement of loading. The initial stiffnesses were almost identical for θ ranging from 45 to 75 deg. When θ was between 0 and 45 deg., the initial stiffness increased with both θ and the value of pf_y. When shearing failures occurred, the ultimate slips were similar to those observed in initially uncracked specimens. Separations began to develop rapidly at three-quarters of the ultimate load, for θ between 0 and 30 deg. For θ equal to 45 deg., separations did not develop until immediately prior to collapse, while for angles θ of 60 and 75 deg. only contractions occurred. Separations at ultimate were as large as 0.06 in. (1.52 mm).

The ultimate shear strengths of the modified push-off specimens which had shearing type failures are compared in Fig. 6 with results from the push-off tests of Series 1, 2 and 3. In this figure the data from Series 9 and 10 are normalized to a concrete strength f'_c of 4100 psi (288 kgf/cm²), the average concrete strength of the specimens in Series 1 and 2. The values of applied normal stress σ_{Nx} and of v_u were multiplied by the ratio $4100/f'_c$. The total normal compressive stress across the shear plane is assumed to be equal to $\sigma_{Nx} + pf_y$. Also shown in Fig. 6 is a failure envelope for concrete with a cylinder strength of 4100 psi. The intrinsic shape of this failure envelope was obtained from biaxial tests of concrete reported by Kupfer, Hilsdorf and Rusch[8]. The assumption that σ_{Nx} may be added to pf_y when estimating v_u can be seen to be conservative for all values of σ_{Nx}. Furthermore, under certain conditions, the shear strength can be as large as the intrinsic strength of the concrete. This occurred when $\sigma_{Nx} + pf_y$ was greater than $0.3f'_c$ and the ratio of σ_{Nx} to pf_y was simultaneously greater than 1.3. (An initially cracked specimen having σ_{Nx}/pf_y equal to 2.6, but with $\sigma_{Nx} + pf_y$ of only $0.2f'_c$ developed a strength almost identical with that of a simple push-off specimen having pf_y equal to $0.2f'_c$.)

Further investigations are needed to define completely the effect on shear transfer strength of the ratio of σ_{Nx} to pf_y, of direct tensile stresses acting transverse to the shear plane, and of applying the shearing force after the direct stress has been increased to its maximum value.

Hypotheses for behavior

Shear transfer behavior of initially uncracked concrete with reinforcement normal to the shear plane. External loads are assumed to cause a shear stress v along the shear plane and direct stresses σ_{Ny} and σ_{Nx} parallel to and normal to the shear plane, respectively. As loading begins the concrete is uncracked; the transverse reinforcement A_{vf} is unstressed and therefore does not contribute an additional direct stress across the shear plane.

Several short diagonal tension cracks will occur along the length of the shear plane and inclined to it at an angle α when, under increasing shear, the principal tensile stress in the concrete becomes equal to the tensile strength of the concrete. The angle α will depend upon the particular combination of v, σ_{Nx} and σ_{Ny} existing at the time of cracking. In push-off tests without additional externally applied direct stress σ_{Nx}, α is usually about 45 deg.

When the shear load is further increased a truss action develops, as shown in Fig. 7(a). Diagonal struts of concrete are formed by the short, parallel diagonal tension cracks. When the shear acts on the truss, the struts tend to

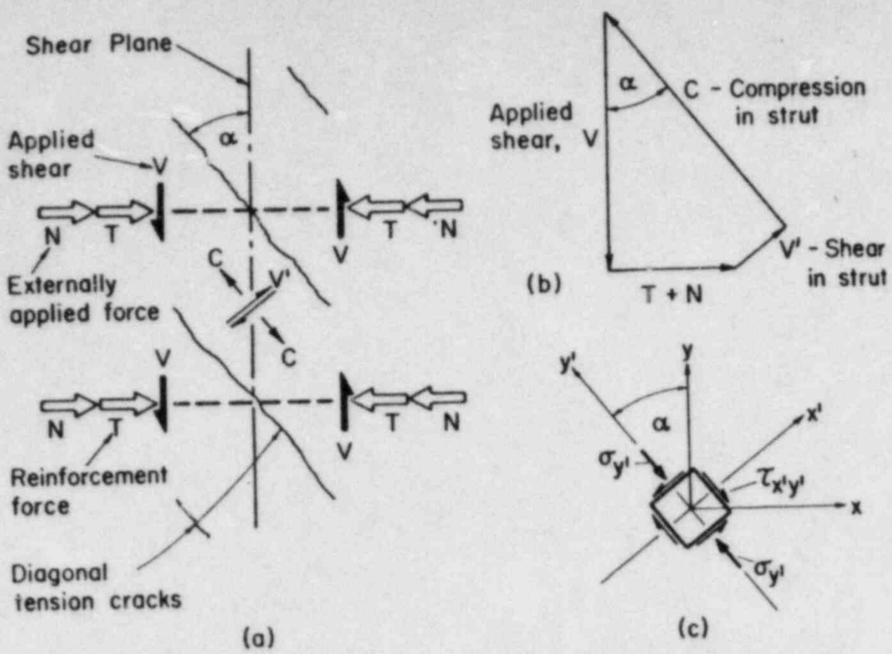

Fig. 7. Shear transfer in initially uncracked concrete

rotate and so stress the transverse reinforcement. Because the diagonal struts are continuous with the concrete on both sides of the shear plane, there will be both compression and transverse shear in the strut. The applied shear is therefore resisted by the components of the strut compression and shear forces acting parallel to the shear plane, as shown in Fig. 7(b).

The reinforcement crossing the shear plane will eventually develop its yield strength $A_{vf}f_y$, provided a failure of the concrete does not occur first. Failure will finally occur when the concrete struts fail under the combined action of compression and shear in the struts, while the reinforcement continues to develop its yield strength.

Consider an element of concrete lying in the shear plane, at the middle of the thickness of a strut. With reference to coordinates x' and y', the stresses acting on the element will be as shown in Fig. 7(c). They comprise a compression $\sigma_{y'}$ acting parallel to the direction of the diagonal tension cracks, and shear stresses $\tau_{x'y'}$ oriented as shown. Because the faces of the strut formed by the diagonal tension cracks are unloaded free surfaces, $\sigma_{x'}$ is zero. The pairs of values of $\sigma_{y'}$ and $\tau_{x'y'}$ at failure of the concrete can be obtained from the failure envelope for the concrete using the geometrical construction shown in Fig. 8. A succession of Mohr circles is drawn tangent to the failure envelope. The intersection of any particular circle and the τ axis will define the point ($\sigma_{x'}$, $\tau_{x'y'}$), since $\sigma_{x'}$ is zero. The diametrically opposite point on the circle must therefore be the point ($\sigma_{y'}$, $\tau_{x'y'}$), where $\sigma_{y'}$ and $\tau_{x'y'}$ are a pair of stresses corresponding to failure of the concrete.

The state of stress in the element on the shear plane can also be expressed as σ_x, σ_y and τ_{xy} with respect to the axes x and y, normal and parallel to the shear plane, respectively. These stresses can be stated in terms of $\sigma_{y'}$ and $\tau_{x'y'}$ as follows:

$$\sigma_x = \sigma_{y'} \sin^2 \alpha - 2\tau_{x'y'} \sin \alpha \cos \alpha \quad (1)$$

$$\sigma_y = \sigma_{y'} \cos^2 \alpha + 2\tau_{x'y'} \sin \alpha \cos \alpha \quad (2)$$

$$\tau_{xy} = -\sigma_{y'} \sin \alpha \cos \alpha + \tau_{x'y'} (\cos^2 \alpha - \sin^2 \alpha) \quad (3)$$

If $\alpha = 45$ deg., then

$$\sigma_x = \frac{\sigma_{y'}}{2} - \tau_{x'y'} \quad (1a)$$

$$\sigma_y = \frac{\sigma_{y'}}{2} + \tau_{x'y'} \quad (2a)$$

$$\tau_{xy} = -\frac{\sigma_{y'}}{2} \quad (3a)$$

Since pairs of values of $\sigma_{y'}$ and $\tau_{x'y'}$ corresponding to failure of the concrete can be obtained as shown in Fig. 8, it is possible to calculate values of σ_x, σ_y and τ_{xy} which correspond to failure of the concrete.

Now at failure, σ_x is the direct stress acting across the shear plane as a result of the shear transfer reinforcement being stressed to yield, plus any externally applied direct stress σ_{Nx} act-

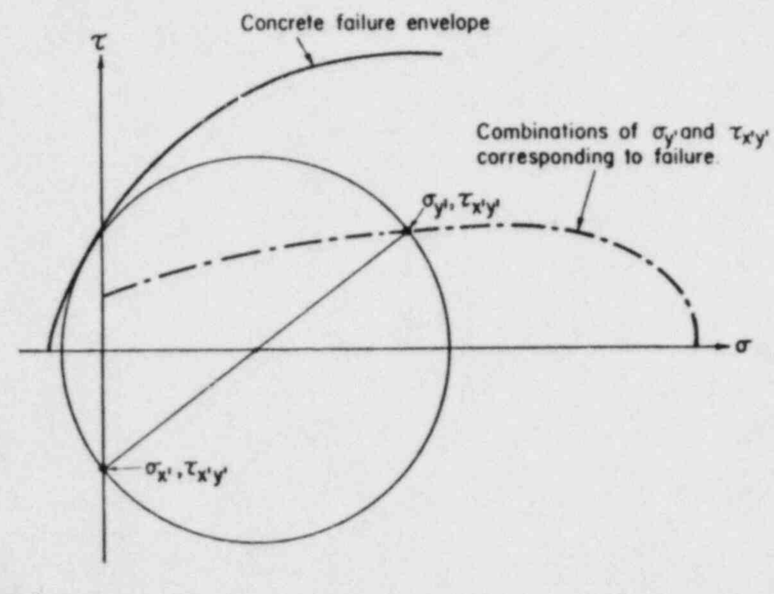

Fig. 8. Derivation of combinations of $\sigma_{y'}$ and $\tau_{x'y'}$ which cause failure of the concrete

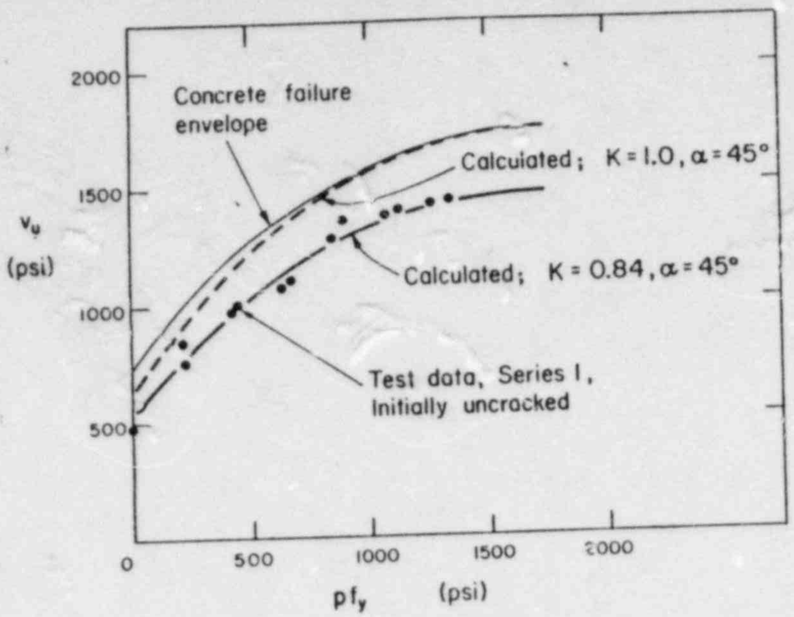

Fig. 9. Comparison of calculated and test shear transfer strengths of initially uncracked push-off specimens

ing across the shear plane at failure, i.e.,

$$\sigma_x = \frac{A_{vf} f_y}{bd} + \sigma_{Nx} = pf_y + \sigma_{Nx} \quad (4)$$

Where A_{vf} is the total cross-sectional area of shear transfer reinforcement, and f_y its yield strength. Also, τ_{xy} is the shear stress in the shear plane, at the center of a strut. We may then write,

$$v_u = \frac{v_u}{bd} = K\tau_{xy} \quad (5)$$

Hence if $\alpha = 45$ deg., then $v_u = -K\sigma_y'/2$ and $pf_y + \sigma_{Nx} = (\sigma_y'/2 - \tau_{x'y'})$. The value of the coefficient K would be 1.0 if the shear stresses were uniformly distributed across the strut, and could be as low as 0.67 if the shear stress distribution across the strut were parabolic. When the external normal stress σ_{Nx} is zero or small, the concrete struts must rotate slightly in order to strain the transverse reinforcement. This causes the ends of the diagonal tension cracks to propagate parallel to the shear plane for a short distance. As a result, the shear stress in the strut is increased locally to a value higher than the average shear stress v_u based on the total area of the shear plane. Failure then tends to shift from the shear plane to a parallel plane containing the ends of the cracks, and occurs when the locally higher shear stress reaches a critical value. The diagonal struts at each end of the shear plane may be incomplete, depending on the exact location of the diagonal tension cracks. In an extreme case this could reduce the total effective cross-section resisting shear by an amount equal to the width of the shear plane multiplied by the projected length on the shear plane of a single diagonal tension crack. Both of the foregoing types of behavior can be expected to result in K becoming less than 1.0.

Using Eqs. (1) and (3) it is therefore possible to calculate pairs of values of $(pf_y + \sigma_{Nx})$ and v_u corresponding to shear transfer failure, provided some value can be assigned to the coefficient K. The actual distribution of shear stress across each strut will probably be intermediate between the uniform and parabolic distributions. In Fig. 9 the calculated relationship between v_u and pf_y, corresponding to an average value of 0.84 for K and the assumption that angle α is 45 deg., is seen to be in reasonably close agreement with results obtained in push-off tests of initially uncracked specimens in which σ_{Nx} was zero. Also shown are the relationship between v_u and pf_y corresponding to a value of 1.0 for K, and the failure envelope used in the calculations. The intrinsic shape of the failure envelope was obtained from biaxial tests of concrete reported by Kupfer, Hilsdorf and Rusch[8]. Use was made of data reported for a concrete having a ratio of tensile to compressive strength corresponding to that of the concrete used in the push-off specimens, $(f_t/f_c' = 1/12.33)$.

The results of the modified push-off tests in which the ratio of σ_{Nx} to pf_y is greater than 1.3 agree reasonably well with calculations assuming $K = 1.0$. In this case the ends of the cracks do not propagate parallel to the shear plane, and therefore the total cross section of the shear plane acts to resist the applied shear.

In the pull-off specimens a direct tensile stress existed parallel to the shear plane at the time of diagonal tension cracking. The intensity of the direct tensile stress was half the intensity of the shear stress. The diagonal tension crack angle α which corresponds to this is 52 deg. This increase in the crack angle from 45 to 52 deg. would lead to a reduction in calculated strength of about 10 percent, other characteristics remaining the same. The actual reduction found in the pull-off tests was greater than this, indicating that the K value is less in the pull-off specimen than in the push-off specimen. The extension of the ends of the diagonal tension cracks parallel to the shear plane was more marked in the pull-off tests than in the push-off tests. For a given applied shear, this would increase the local intensity of shear stress in the pull-off specimen. This increase would result in failure at a lower average shear stress, corresponding to a reduction in the value of K.

Shear transfer behavior of initially cracked concrete with reinforcement normal to the shear plane. When an initially cracked specimen is loaded in shear, slip will occur along the shear plane. The faces of the crack are rough and hence when slip occurs, the crack faces are forced to separate. This separation causes tension strains in the reinforcement crossing the shear plane. The tension force so induced in the reinforcement is balanced by an equal compression force acting across the crack. This compression force produces a frictional resistance to sliding between the faces of the crack, thus opposing the applied shear. The relative movement of the concrete on opposite sides of the crack also subjects the individual reinforcing bars to a shearing action. The resistance of the bars to this shearing action, sometimes referred to as dowel action, also contributes to the shearing resistance.

In an under-reinforced shear plane, the separation of the crack faces is eventually sufficient to strain the reinforcement to its yield point. At ultimate strength therefore, the compression force across the crack is equal to the yield strength of the reinforcement $A_{vf}f_y$. The frictional resistance to shear along the crack is then equal to this force multiplied by the coefficient of friction for concrete. In addition to the frictional resistance to shear, there is also shear resistance due to the dowel action of the reinforcement crossing the crack in the shear plane, and the resistance to shearing off of asperities projecting from the faces of the crack. It is hypothesized that the frictional resistance to sliding and the reinforcement dowel effect are the principal contributors to shear resistance. This view is supported by the fact that for values of pf_y greater than 200 psi (14 kgf/cm²), the slope of the curve relating v_u and pf_y is equal to the coefficient of friction between formed concrete surfaces measured by Gaston and Kriz[9]. Further, when the dowel action was destroyed in two initially cracked push-off specimens (Series 6), the shear strength dropped almost to that which could be provided by friction alone. In these specimens the reinforcement became kinked at ultimate, and hence a component of the reinforcement force acted along the shear plane. It is thought that the excess strength of these specimens above the frictional resistance was due to this kinking effect.

The concrete strength does not appear to affect the shear transfer strength of an initially cracked under-reinforced specimen. This is consistent with the shear strength being primarily developed by friction, since the coefficient of friction is independent of the concrete strength. The behavior hypothesis also explains why the shear transfer strength of initially cracked pull-off and push-off specimens are the same for the same value of the reinforcement parameter pf_y. Direct stresses parallel to the shear plane will not affect either the frictional resistance to sliding along the shear plane, or the dowel effect. Hence a change in this longitudinal direct stress from tension to compression does not affect the shear transfer strength in this case.

In a heavily reinforced shear plane, or one subject to a substantial externally applied normal compressive stress, it is possible for the theoretical shear resistance due to friction and dowel effects to become greater than the shear which would cause failure in an initially uncracked specimen having the same physical characteristics. In such a case, the crack in the shear plane "locks up" and the behavior and ultimate strength then become the same as for an initially uncracked specimen. When this occurs, the shear strength becomes dependent upon the concrete strength, whereas before it was independent. This change in behavior corresponds to the change in slope of the v_u/pf_y curve for 2500 psi (176 kgf/cm²) concrete in Fig. 4. In Fig. 2 it can also be seen that at the highest values of pf_y, the strengths of both initially cracked and initially uncracked specimens are the same.

In a moderately to heavily reinforced shear plane, diagonal tension cracks may form at angle α to the shear plane, but failure still occurs by sliding along the crack in the shear plane at an ultimate shear strength less than that of the corresponding initially uncracked specimen.

Shear transfer in design

Section 11.15 of the *ACI Building Code*, ACI 318-71[10], allows design for shear transfer to be based on the "shear-friction" hypothesis proposed by Birkeland[1] and Mast[2]. This is a simplification for design purposes of the

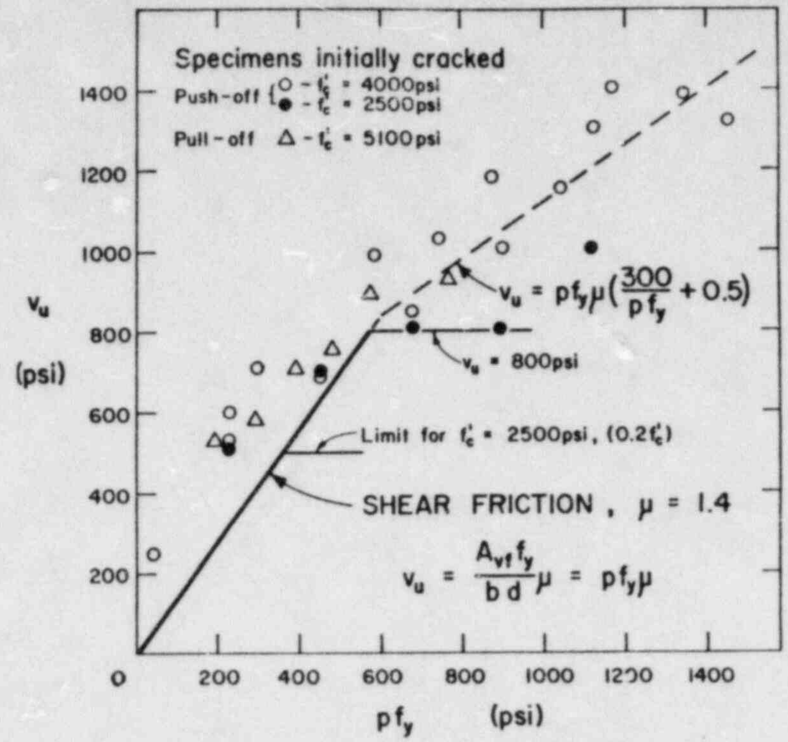

Fig. 10. Comparison of shear transfer strength calculated using the shear friction provisions of ACI 318-71 with measured strengths of initially cracked push-off and pull-off specimens

hypothesis for the behavior of initially cracked concrete described above. In the shear-friction approach, it is assumed that for some unspecified reason a crack exists in the shear plane. The shear resistance is then assumed to be developed entirely by the frictional resistance to sliding of one crack face over the other, when acted upon by a normal force equal to the yield strength of the reinforcement crossing the shear plane. A fictitiously high value of the coefficient of friction μ is used to compensate for neglect of dowel action and other factors. For a crack in monolithic concrete, μ is taken as 1.4. For conservative calculation of strength, the shear transfer strength is limited to $0.2f'_c$ or 800 psi (56 kgf/cm²) whichever is the less. The shear-friction equation may be written as

$$v_u = \frac{A_{vf}f_y}{bd}\mu = pf_y\mu \qquad (6)$$

but not more than $0.2f'_c$ or 800 psi.

In Fig. 10 the shear transfer strength calculated according to Eq. (6) is indicated by unbroken lines and is com-

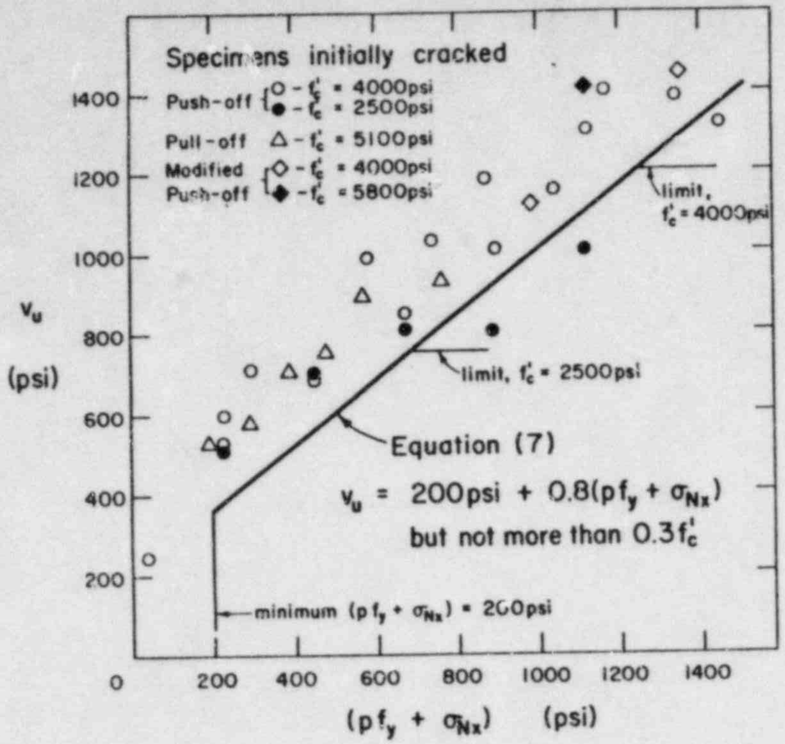

Fig. 11. Comparison of shear transfer strength calculated using Eq. (7) with the measured strengths of initially cracked push-off, pull-off and modified push-off specimens

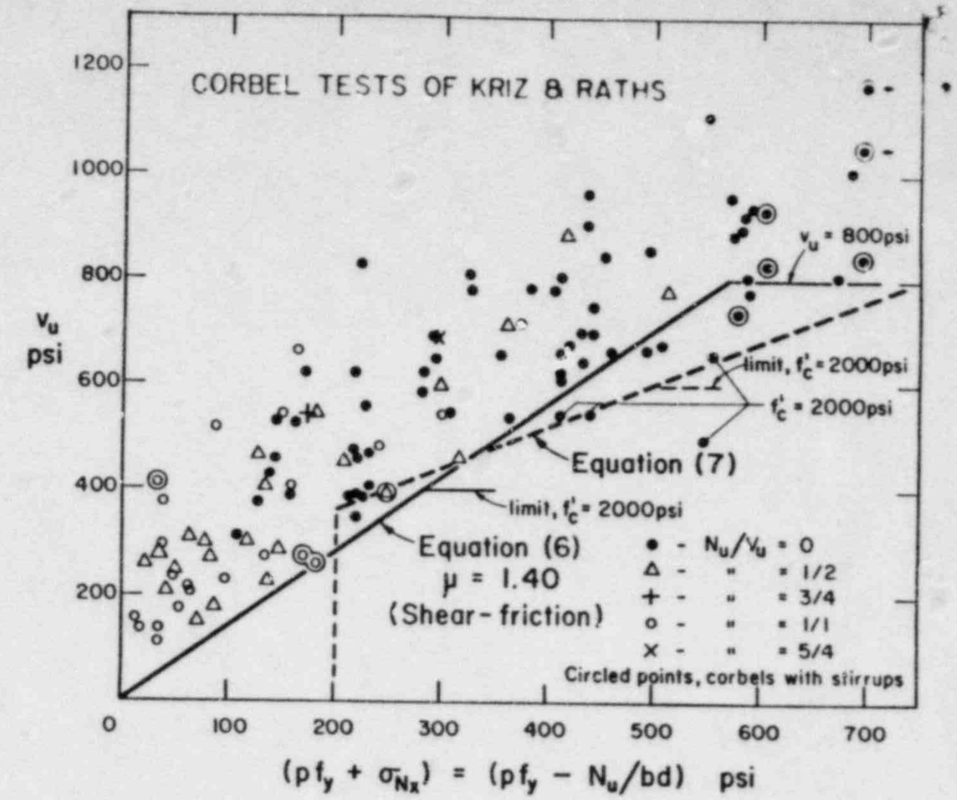

Fig. 12. Comparison of the shear strength of corbels calculated using Eqs. (6) and (7) with the measured strengths of tested corbels

pared with the measured strength of all the initially cracked push-off and pull-off specimens tested in the program reported here. It can be seen that the provisions of ACI 318-71 yield a conservative estimate of the shear transfer strength of concrete cracked along the shear plane. However, it is also clear that shear stresses considerably in excess of the arbitrary upper limit of 800 psi (56 kgf/cm²) can be developed if appropriate reinforcement is provided and the concrete strength is high enough. Section 6.1.9 of the *PCI Design Handbook*(11) suggests that this reinforcement may be designed using Eq. (6), providing that μ is multiplied by $(300/pf_y + 0.50)$ when pf_y exceeds 600 psi (42 kgf/cm²). This proposal is indicated by the broken line in Fig. 10. It can be seen that this proposal is in accord with the trend of the experimental data for concrete strengths greater than 2500 psi (176 kgf/cm²) and for shear strengths less than about 1300 psi (91 kgf/cm²). A deficiency in this proposal is that no upper limit on either pf_y or v_u is specified.

An alternate approach, simpler to apply in design, would be the use of the following equation for shear transfer across a crack in monolithic concrete

$$v_u = 200 \text{ psi} + 0.8\,(pf_y + \sigma_{Nx}) \qquad (7)$$

with the restrictions that v_u shall be not more than $0.3f'_c$ and $(pf_y + \sigma_{Nx})$ shall be not less than 200 psi (14 kgf/cm²). σ_{Nx} is the externally applied direct stress acting across the shear plane, taken as positive for a compressive stress and negative for a tensile stress. In Fig. 11, Eq. (7) is compared with the measured strength of all the initially cracked specimens tested in the program reported here and is seen to be a lower bound to the data. Eq. (7) is slightly less conservative than Eq. (6) for $(pf_y + \sigma_{Nx})$ less than 333 psi (23 kgf/cm²) and slightly more conservative for values of $(pf_y + \sigma_{Nx})$ between 333 and 572 psi (23 and 40 kgf/cm²), the limit of applicability of Eq. (6) according to ACI 318-71.

The results reported here validate Eq. (7) for values of $(pf_y + \sigma_{Nx})$ up to 1400 psi (99 kgf/cm²), when σ_{Nx} is zero or compressive. The results reported by Kriz and Raths[12] for corbels subjected to shear and to tension forces in the direction of the reinforcement, indicate that there are a wide variety of conditions for which Eq. (7) is also valid for values of σ_{Nx} which are tensile. In Fig. 12 Eqs. (6) and (7) are compared with data from Kriz' and Raths' corbel tests. In plotting Fig. 12, v_u was taken as the nominal shear stress at yield of the tension reinforcement, or at ultimate strength of the corbel if the yield of the tension reinforcement did not occur. In accordance with Kriz' and Raths' findings and as required by Section 11.14 of ACI 318-71, the reinforcement ratio p was taken as $(A_s + A_h)/bd$ when shear only acted on the corbel and as A_s/bd when both shear V_u and tension N_u acted on a corbel. In this latter case, $\sigma_{Nx} = N_u/bd$. It can be seen that, providing the limitations placed on them are observed, both Eqs. (6) and (7) yield conservative estimates of the ultimate strength of corbels. (The corbel tests considered included specimens for which the ratio of the tensile stress σ_{Nx} to the shear stress v_u varied from 0 to 1.25, and for which the ratio of moment acting on the corbel to the shear times the effective depth at the column face (a/d) varied from 0.11 to 0.62. The maximum value of $(pf_y - N_u/bd)$ was 514 psi (36 kgf/cm²), and the maximum value of pf_y considered was 700 psi (49 kgf/cm²).

Conclusions

Concerning design.

1. Within their range of applicability, the shear-friction provisions of ACI 318-71 yield a conservative estimate of the shear transfer strength of reinforced concrete whether or not a crack exists in the shear plane.

2. Higher shear transfer strengths than the upper limit of 800 psi (56 kgf/cm²) specified in ACI 318-71 can be developed if appropriate reinforcement is provided and the concrete strength is adequate. Such reinforcement may be proportioned using Eq. (7).

Concerning fundamental behavior.

1. A pre-existing crack along the shear plane will both reduce the ultimate shear transfer strength and increase the slip at all levels of load. 1

2. Changes in strength, size, and spacing of reinforcement affect the shear transfer strength only insofar as they change the value of the reinforcement parameter pf_y for $f_y \leq 66$ ksi (4640 kgf/cm²).

3. In initially cracked concrete, the concrete strength sets an upper limit value for pf_y below which the relationship between v_u and pf_y is independent of concrete strength. Above this value of pf_y, the shear transfer strength increases at a much reduced rate for lower strength concrete and is equal to that of similarly reinforced, initially uncracked concrete.

4. Direct tension stresses parallel to the shear plane reduce the shear transfer strength of initially uncracked concrete, but do not reduce the shear transfer strength of concrete initially cracked in the shear plane.

5. An externally applied compressive stress acting transversely to the shear plane is additive to pf_y in calculations of the ultimate shear transfer strength of both initially cracked and uncracked concrete.

6. The shear transfer strength of initially uncracked concrete is developed by a truss action after diagonal tension cracking. Failure occurs when the inclined concrete struts fail under a combination of shear and axial force.

7. The shear transfer strength of initially cracked concrete with moderate amounts of reinforcement is developed primarily by frictional resistance to sliding between the faces of the crack and by dowel action of the reinforcement crossing the crack. When large amounts of reinforcement, or sufficient externally applied compression stresses normal to the shear plane are provided, then the crack in the shear plane "locks up" and shear transfer strength is developed as in initially uncracked concrete. 7

Acknowledgments

This study was carried out in the Structural Research Laboratory of the University of Washington, Seattle. It was made possible by the support of donors to the Structural Concrete Research Fund at the University of Washington, and by the Bethlehem Steel Corporation who donated reinforcing bars.

References

1. Birkeland, P. W. and Birkeland, H. W., "Connections in Precast Concrete Construction," *Journal of the American Concrete Institute*, Vol. 63, No. 3, March 1966, pp. 345-368.
2. Mast, R. F., "Auxiliary Reinforcement in Concrete Connections," *Proceedings, ASCE*, Vol. 94, ST6, June 1968, pp. 1485-1504.
3. Hofbeck, J. A., Ibrahim, I. O. and Mattock, A. H., "Shear Transfer in Reinforced Concrete," *Journal of the American Concrete Institute*, Vol. 66, No. 2, Feb. 1969, pp. 119-128.
4. Chatterjee, P. K., "Shear Transfer in Reinforced Concrete," MSCE Thesis, University of Washington, Seattle, June 1971.
5. Vangsirirungruang, K., "Effect of Normal Compressive Stresses on Shear Transfer in Reinforced Concrete," MSCE Thesis, University of Washington, Seattle, July 1971.
6. Zia, P., "Torsional Strength of Prestressed Concrete Members," *Journal of the American Concrete Institute*, Vol. 57, No. 10, April 1961, pp. 1337-1359.
7. Anderson, A. R., "Composite Designs in Precast and Cast-in-Place Concrete," *Progressive Architecture*, Vol. 41, No. 9, September 1960, pp. 172-179.
8. Kupfer, H., Hilsdorf, H. K. and Rusch, H., "Behavior of Concrete Under Biaxial Stresses," *Journal of the American Concrete Institute*, Vol. 66, No. 8, Aug. 1969, pp. 656-666.
9. Gaston, J. R. and Kriz, L. B., "Connections in Precast Concrete Structures—Scarf Joints," *Journal of the Prestressed Concrete Institute*, Vol. 9, No. 3, June 1964, pp. 37-59.
10. "Building Code Requirements for Reinforced Concrete (ACI 318-71)," American Concrete Institute, Detroit, Mich., 1971.
11. "PCI Design Handbook," Prestressed Concrete Institute, Chicago, Ill., 1971.
12. Kriz, L. B. and Raths, C. H., "Connections in Precast Concrete Structures—Strength of Corbels," *Journal of the Prestressed Concrete Institute*, Vol. 10, No. 1, Feb. 1965, pp. 16-61.

Discussion of this paper is invited.
Please forward your discussion to PCI Headquarters by July 1 to permit publication in the July-August 1972 issue of the PCI JOURNAL.